THE ROLE OF CHOLESTEROL IN MU-OPIOID RECEPTOR-MEDIATED ADENYLYL CYCLASE SENSITIZATION

Jason C. Chen

Traynor Lab, Department of Pharmacology
University of Michigan Medical School

April 21, 2009
Honors Thesis in Biochemistry

This thesis has been read and approved by 
Date: 4 / 17 / 09

Table of Contents

Abstract

Chronic agonist treatment of opioid receptors causes sensitization of adenylyl cyclase (AC), which is characterized by an increased basal level of AC activity, and can be observed as a cAMP overshoot upon re. While the mechanisms behind sensitization are still unknown, recent studies have shown that G protein-coupled receptors and associated signaling elements are localized in cholesterol-enriched membrane microdomains called lipid rafts. In order to investigate the role of cholesterol and lipid rafts in AC sensitization, we used C6 cells stably expressing the mu-opioid receptor (C6μ). Chronic treatment of C6μ cells using selective mu-opioid agonist DAMGO ([D-Ala^2, N-MePhe^4, Gly-ol]-enkephalin) and morphine was used to sensitize AC. Depletion of cellular cholesterol using the cholesterol-sequestering agent methyl-β-cyclodextrin (MβCD) prior to sensitization of AC caused a significant decrease in the forskolin-stimulated cAMP production, which could be recovered by the inclusion of cholesterol with MβCD. Cholesterol depletion after sensitization, on the other hand, had no effect on overshoot, suggesting that the development and expression of overshoot utilize different biochemical pathways. Further investigation using isolated lipid raft and non-raft membranes from C6μ cells demonstrated that mu-receptors are localized in lipid rafts and associate with cholesterol throughout the plasma membrane. AC sensitization experiments using these membranes also supported our conclusions from the whole cells studies. Together, our findings suggest that lipid rafts and membrane cholesterol have important roles in mu-opioid receptor signaling and cellular responses to chronic opioid exposure.

Introduction and Background

Opioids have been used for over six millennia for their potent analgesic properties, and remain one of the most widely-used classes of painkillers. However, the potential benefits of opioids have been overshadowed by their tendency to cause tolerance and dependence after prolonged use.

While there are three major types of opioid receptors (mu, delta and kappa), mu-opioid receptors and mu agonists are of particular interest because they exhibit the strongest analgesic effects and substance abuse potential. Upon stimulation by an agonist (e.g. morphine), opioid receptors activate heterotrimeric G proteins (Gα and Gβγ subunits) and initiate an intracellular signaling cascade (Figure 1).

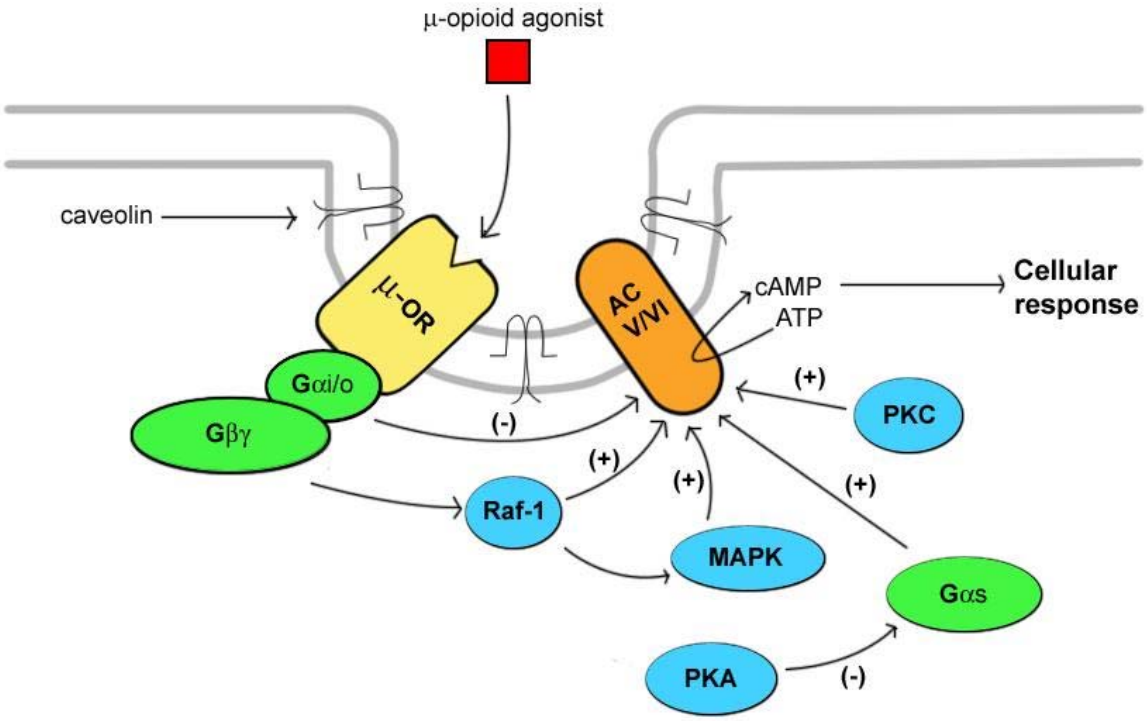

Figure 1. Opioid receptor signaling pathways that affect adenylyl cyclase and are implicated in the sensitization of adenylyl cyclase after chronic agonist treatment. The mu-opioid receptor (μ-OR) modulates AC activity through Gα and Gβγ subunits, which dissociate upon agonist exposure. $G\alpha_{i/o}$ subunits inhibit AC while $G\alpha_s$ subunits stimulate AC and are

thought to be up-regulated during sensitization (1). PKA can be localized with caveolin and has been shown to have inhibit $G\alpha_s$ (2). $G\beta\gamma$ subunits signal to various downstream effectors, including Raf-1 and elements of the mitogen-activated protein kinase (MAPK) signaling pathway (2). Stimulation of PKC causes translocation of PKC to caveolae and an enhancement of AC activity (1,3). Despite the diagram above which suggests that $G\beta\gamma$ has a stimulatory role, $G\beta\gamma$-regulated signaling events are complex and their exact role in sensitization of AC remains undetermined.

One down stream effector is adenylyl cyclase (AC), which is inhibited by G proteins coupled to opioid receptors, including $G\alpha_{i/o}$ (1). However, under chronic opioid agonist treatment, adenylyl cyclase becomes sensitized (also called superactivation or supersensitization). Upon withdrawal of opioid agonist and thus removal of inhibition from the G protein cascade, sensitized AC produces more cAMP when activated. This increased activity is called overshoot, measured as the cAMP accumulation under direct stimulation of AC and in the presence of a saturating quantity of a mu opioid antagonist such as naloxone. Sensitization is hypothesized to be the result of adaptation to continual drug exposure and is a cellular model of withdrawal.

Although G proteins and effector molecules are relatively abundant in cells, the speed and specificity of GPCR signaling suggest that the localization of elements within the membrane might have a significant role in secondary messenger formation (4). Lipid rafts, membrane microdomains rich in cholesterol and sphingomyelin, are of particular interest in the field of GPCR signaling. One specialized type of lipid rafts are caveolae, which are membrane invaginations associated with the cholesterol binding caveolin (5). Caveolin can therefore be used as a marker when studying lipid rafts. While opioid receptors and their signaling components can be found throughout the plasma membrane, recent studies have demonstrated the importance of lipid rafts to the mu-opioid signaling pathway. There is evidence that certain isoforms of AC inhibited by $G\alpha_{i/o}$ and involved in sensitization (AC5 and AC6) are localized in lipid rafts (1,6). In addition, there is evidence that proteins involved in sensitization, such as $G\alpha_{i/o}$

and Gβγ (7) move into detergent-resistant (raft) membranes upon activation. Raf-1, a kinase postulated to be involved in sensitization, migrates to cholate-insoluble (raft) fractions following activation by epidermal growth factor and associates with caveolin (8). Confocal microscopy studies by Zheng et al. (9) and our laboratory have shown that mu opioid receptors colocalize with lipid rafts in stably transfected HEK293 cells. There is also evidence that chronic treatment with opioid agonist etorphine induces a translocation of mu opioid receptors and $G\alpha_i$ from raft to non-raft domains (9). Finally, disruption of lipid rafts using methyl-β-cyclodextrin (for cholesterol depletion) has been shown to affect AC sensitization, observed by a decrease in overshoot according to unpublished results from our lab and others (6). Because of the evidence supporting the role of lipid rafts in AC sensitization, we were interested in how disruption of lipid rafts can have differential effects on the two phases of sensitization: development and expression (Figure 2).

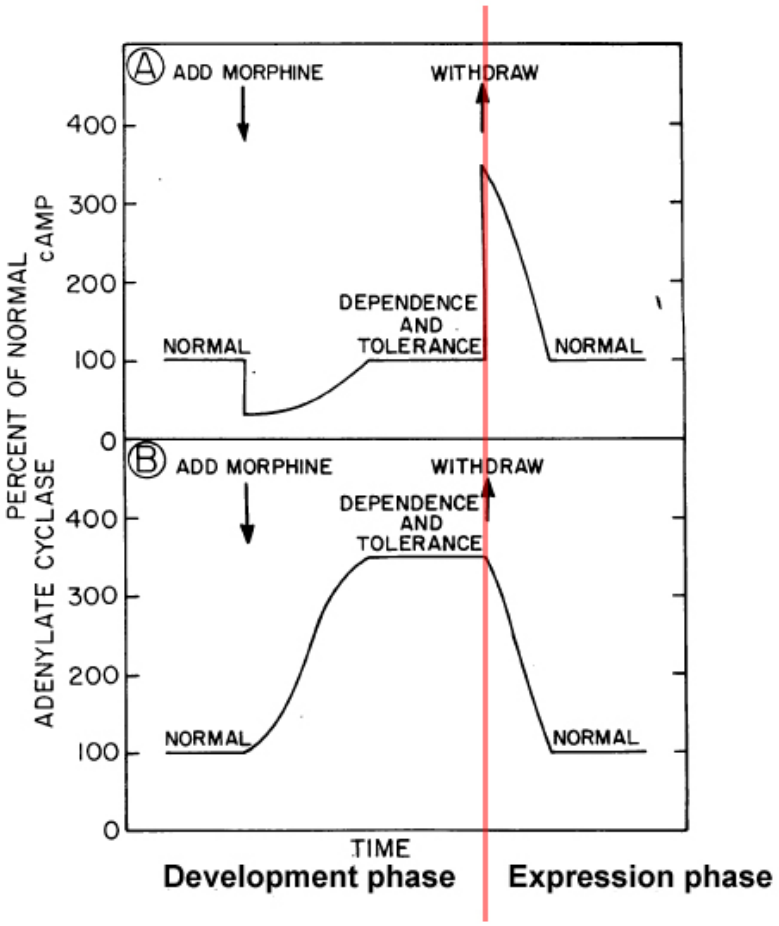

Figure 2. Summary of changes in adenylyl cyclase activity and cAMP production at different stages in the development and expression phases of overshoot. Addition of an agonist (morphine) causes an initial decrease cAMP production which returns to normal levels as AC adapts to chronic inhibition via up-regulation of activity. This process is called the development phase of sensitization. During withdrawal, direct stimulation of AC using forskolin and removal of morphine causes a sharp increase in cAMP production that is significantly higher than normal levels. In the absence of chronic inhibition by morphine, AC activity levels return to normal levels. This process is called the expression phase of overshoot.

We report here that depletion of cholesterol using methyl-β-cyclodextrin significantly affects the development, but not the expression of AC overshoot. Depletion of cholesterol had a negligible effect on short-term AC inhibition, suggesting that inhibition and overshoot work through different biochemical pathways.

In order to better clarify the role of lipid rafts in AC signaling without using MβCD, which may have non-specific effects, we attempted to isolate lipid raft membrane fractions that retained the function of membrane proteins such as AC. Most lipid raft isolation methods take advantage of the detergent-resistant property of these cholesterol-enriched domains in order to isolate raft fractions for further biochemical studies. These methods typically use ultracentrifugation using sucrose gradients in combination with nonionic detergents such as Triton X-100 (10,11), Lubrol WX and CHAPS (12) in order to separate cellular components and solubilize non-raft membrane fractions. However, detergents have been known to eliminate the activity of membrane proteins. Fractions isolated via these methods also may give misleading results for several reasons, including the creation of "detergent-resistant" aggregates rather than native lipid rafts (13). There is also evidence that Triton X-100 may solubilize some raft-associated proteins and that different detergents produce rafts with varying cholesterol and protein composition (14). One non-detergent protocol was developed by Song et al. that utilized sodium bicarbonate and high pH to solubilize non-raft membranes. However, this method is relatively long (16-20 hours), which may affect membrane protein activity and have undesired effects on secondary messenger signaling. As a result, we decided to focus on a non-detergent protocol developed by Smart et al. using several Percoll and Optiprep gradient spin steps rather than traditional sucrose gradients (15). Under these relatively milder conditions, Smart et al. report that raft integrity is preserved and purification of caveolae is improved. However, the protocol outlined by Smart et al. still requires 3 lengthy centrifugation steps, which decreases overall protein yields in the resulting fractions. Because our objective is to evaluate the functionality of lipid rafts through various assays, we require a protocol that is relatively quick and produces high yields, while maintaining membrane integrity and purity of separated

fractions. Therefore, we modified the Smart et al. protocol to decrease the time needed to complete the membrane separation, increase the purity of raft fractions and improve the recovery of raft-associated proteins (15).

Materials and Methods

Materials

Morphine, DAMGO ([D-Ala^2, N-MePhe^4, Gly-ol]-enkephalin) and naloxone were obtained through the Narcotic Drug and Opioid Peptide Basic Research Center at the University of Michigan (Ann Arbor, MI). [^{3}H]diprenorphine and [^{35}S]GTPγS were obtained from Perkin-Elmer Life Sciences (Boston, MA). Bicinchoninic acid (BCA) protein assay kits, SuperSignal West Pico chemiluminescent substrate (for enhanced chemiluminescence) and nitrocellulose membranes were obtained from Pierce Biotechnology (Rockford, IL). Tissue culture media, fetal bovine serum and Amplex Red Cholesterol Assay Kits were obtained from Invitrogen (Carlsbad, CA). Optiprep was from Accurate Chemical and Scientific (Westbury, NY). Anti-phospho-p44/42 MAPK (ERK1/2) antibody and anti-p44/42 MAPK (ERK1/2) antibody were from Cell Signaling Technology, Inc. (Beverly, MA); anti-transferrin receptor antibody was from Invitrogen (Carlsbad, CA); anti-β-actin antibody and anti-α-tubulin antibody were from Sigma-Aldrich (St. Louis, MO); anti-prohibitin was from Fisher Scientific (Pittsburgh, PA); anti-EEA1 (Early Endosome Antigen 1) antibody and all secondary antibodies were from Santa Cruz Biotechnology (Santa Cruz, CA). All other reagents were obtained from Sigma-Aldrich (St. Louis, MO) unless otherwise stated.

Buffers

The following buffers were used: PBS (0.9% NaCl, 0.61 mM Na_2HPO_4, 0.38 mM KH_2PO_4, pH 7.4), lifting buffer (5.6 mM glucose, 5 mM HEPES, 137 mM NaCl, 1 mM EDTA, 5 mM KCl, pH 7.4), buffer B (250 mM sucrose, 5 mM HEPES, 1 mM EGTA, pH 7.4), TES buffer (120 mM Tris, 0.25 M sucrose, 6 mM EDTA, pH 7.8), GTPγS buffer (50 mM Tris-HCl, pH 7.4, 5 mM $MgCl_2$, 100 mM NaCl), SDS sample buffer (62.5 mM Tris-HCl, pH 6.8, 2% SDS, 10% glycerol, 5% 2-mercaptoethanol, 0.01% bromphenol blue), TBS (20 mM Tris, 140 mM NaCl, pH 7.4). All Optiprep and Percoll solutions were diluted in TES buffer. The Amplex Reaction Buffer used for the Amplex Red Assay contained 0.1 M potassium phosphate, pH 7.4, 0.05 M NaCl, 5 mM cholic acid and 0.1% Triton® X-100

Cell culture

Rat glioma cells (C6) stably transfected with rat mu opioid receptor (C6μ) as described by Clark et al. (16) were grown in Dulbecco's Modified Eagle Medium (DMEM) supplemented with 10% fetal bovine serum (FBS) and 0.8 mg/mL geneticin at 37°C, 5% CO_2. For all experiments utilizing a 24-well plate, cells were first grown to confluence at 37°C in a 10 mL Petri dish, then subcultured 1:50 into the 24-well plate using 0.9 ml trypsin to detach cells, and diluting the cells in DMEM media containing 10% FBS.

Cholesterol depletion and addition

C6μ cells were grown to confluence in 24-well plates in DMEM with 10% FBS. For cholesterol depletion, the media was replaced with serum-free DMEM with or without 4 mM MβCD and incubated at 37°C for 1 hr. For cholesterol addition, the media was replaced with a 8:1 MβCD:cholesterol complex (MβCD-CH) for 2 h at 37°C, created as described by Christian et al. (17). Briefly, cholesterol was dissolved in a glass tube using 1:1 chloroform in methanol and spread as a thin layer coating the inside the tube. Once the solvent had evaporated, serum-free

media containing 4 mM MβCD was added and the solution was vortexed, sonicated for 30 sec, and incubated at 37^{o}C overnight with shaking. Following treatment with MβCD or MβCD-CH, cells were removed from the well with lifting buffer, centrifuged at 4000 rpm for 3 min an IEC Centra CL2 centrifuge and resuspended in 200 μL Amplex reaction buffer for cholesterol and protein analysis.

For MβCD/cholesterol suspensions, 1 mL of warm serum-free DMEM was added to a solution of 50 mg of MβCD and 0.2 mL cholesterol solution (20 mg cholesterol/mL ethanol). The mixture was sonicated for 1 min and centrifuged in National Labnet C-1200 mini-centrifuge for 10 sec. The supernatant (~1 mL) was saved and diluted in 9 mL serum-free DMEM.

Cholesterol and protein determination

Membrane fractions were solubilized using an equivalent volume of Amplex reaction buffer (5mM Na cholic acid, 0.1% Triton X-100, PBS, pH 7.4) for at least 30 min on ice prior to assay. For whole cell cholesterol determination, cells were rinsed with 1 mL PBS, lifted using 1 mL lifting buffer and centrifuged at 4000 rpm for 3 min. The supernatant was discarded and the pellet was resuspended in 200 μL Amplex reaction buffer for at least 30 min on ice prior to assay. Cholesterol was determined using the Amplex Red Cholesterol Assay following the manufacturer's instructions and fluorescence was measured on a Victor2 fluorimeter. Protein was determined using a BCA protein assay kit following the manufacturer's instructions.

Cyclic AMP accumulation assays

C6μ cells were grown to confluence in 24-well plates in DMEM with 10% FBS. To inhibit adenylyl cyclase, media in each well was replaced by 1 mL 10 nM DAMGO in serum-free media containing 5 μM forskolin and 1 mM IBMX (3-Isobutyl-1-methylxanthine) for 10 min. For AC sensitization, cells were treated with 100 nM DAMGO in either serum-free or

serum-containing DMEM for 30 min or overnight, respectively. Cyclic AMP overshoot was then precipitated by 10 μM naloxone, 5 μM forskolin and 1 mM IBMX. The assay was stopped by replacing the media with 1 mL of cold 3% perchloric acid and incubating at 4^{o}C for at least 30 min. A 400 μL aliquot was taken from each well, neutralized with 2.5 M $KHCO_3$, and centrifuged at 13,000 x g for 1 min to pellet precipitate. Cyclic AMP in the supernatant was measured using a cyclic AMP radioimmunoassay kit from GE Healthcare (Buckinghamshire, UK) and following the manufacturer's instructions.

Trypan blue staining

Trypan blue was used to determine the viability of cells via dye exclusion. Cells harvested in lifting buffer were incubated in Trypan blue reagent (1:6 dye:cell vol) for 5 min at room temperature. 10 μL of the suspension was loaded onto a hemocytometer: viable cells remain colorless while dead cells stain blue.

Detergent-free membrane preparation

Membrane fractions were isolated using a modification of the method described by Smart et al. (15). C6μ cells were grown to confluence in two 10 mL Petri dishes and incubated in serum-containing DMEM with or without 100 nM morphine 24 h prior to experiment to sensitize AC. Plates were washed twice with warm PBS after treatment. Cells were harvested in lifting buffer and centrifuged at 1600 rpm for 3 min in an IEC Centra CL2 centrifuge. All subsequent steps were carried out at either 4^{o}C or on ice. The pellet was resuspended in buffer B for a cell concentration of 6% (w/v) and homogenized in a Dounce homogenizer (20 strokes). The homogenate was centrifuged at 2400 rpm for 10 min in a Beckman GPR centrifuge. The postnuclear supernatant (PNS) was removed and transferred to ice. The pellet was resuspended in the same amount of buffer B as in the previous step, and re-centrifuged at 2400 rpm for 10

min. The PNS was removed and combined with the first PNS fraction on ice. Percoll was added to the PNS to attain 12% (w/v) Percoll. The mixture was then centrifuged at 24000 rpm for 30 min in a Beckman L7-55 ultracentrifuge on a Beckman Ti 70.1 rotor. A distinct plasma membrane (PM) band was observed approximately 2/3 from the bottom and was collected with a Pasteur pipette. TES buffer was added to the PM fraction for a total volume of 1.4 mL, and an aliquot was taken for further testing. The remaining PM fraction was homogenized using a Tissue Tearor (Biospec Products, Inc.) at setting 3 for 15 sec and transferred to an 8 mL ultracentrifuge tube. 1 mL of 50% (w/v) Optiprep was added to the top of the homogenized fraction for a final concentration of 23% (w/v) Optiprep. One mL of 12% (w/v) Optiprep was layered on top and the mixture was centrifuged at 22000 rpm for 90 min in a Beckman L7-55 ultracentrifuge on a Beckman Ti 70.1 rotor. Two bands were visible: one above the 23% (w/v) Optiprep layer and one between the 23/12% interface and the bottom of the ultracentrifuge tube. Three fractions were taken: one from above and including the top band ("raft"), one from between the top and bottom bands (middle), and one from everything below and including the bottom band ("non-raft").

Radioligand determination of receptor number

The number of mu opioid receptors in membrane fractions was determined by the method described by Clark et al. (16). Briefly, membrane fractions were homogenized using in a Dounce homogenizer. Membranes were then incubated in 50 mM Tris-HCl, pH 7.4, 4 nM of [^{3}H]diprenorphine and either dH_2O or 50 μM naloxone (for non-specific binding) for 60 min in a shaking water bath at 25^{o}C. Samples were then filtered three times through glass-fiber filters (Whatman GF/C) on a Brandell cell harvester using cold 50 mM Tris, pH 7.4. Radioactivity on

the filters was solubilized in 4 mL of EcoLume scintillation mixture, and counted on a Packard 1500 Liquid Scintillation Counter.

[^{35}S]GTPγS binding assay

[^{35}S]GTPγS binding was performed as described by Clark et al. (16). Briefly, membrane fractions were homogenized using a Dounce homogenizer. Membranes where then incubated in 20 mM Tris-HCl, pH 7.4, 5 mM $MgCl_2$, 100 mM NaCl, 0.1 mM dithiothreitol, 30 μM GDP, dH_2O or 10 μM DAMGO, and 0.1 nM [^{35}S]GTPγS for 60 min in a shaking water bath at 25^{o}C. Samples were filtered four times through glass-fiber filters (Whatman GF/C) on a Brandell cell harvester using cold GTPγS buffer. Filters were dried and EcoLume scintillation cocktail was added. Filters were then heat sealed in polyethylene bags and radioactivity on the filters was counted in a Wallac 1450 MicroBeta Liquid Scintillation and Luminescence Counter.

Western immunoblotting (SDS-PAGE)

Samples were mixed with an equivalent volume of 2x SDS sample buffer, sonicated for 20 sec and boiled for 5 min. Proteins were separated on a 12% polyacrylamide gel using the method of Laemmli (18) on a Bio-Rad Mini-Protean II Electrophoresis Cell with wells loaded for equal protein as measured by BCA protein assay. Proteins were transferred to nitrocellulose membranes, washed in TBS, and blocked using 5% nonfat milk in TBS-0.05% Tween (0.5 mL Tween/1 L TBS) for 1 h at room temperature. Membranes were washed with TBS-Tween and incubated in primary antibody overnight at 4^{o}C. After washing with TBS-Tween, membranes were incubated in secondary antibody for 1 h at room temperature.

Primary antibody dilution	**Secondary antibody dilution**
1:300 anti-prohibitin	1:5000 anti-mouse HRP

1:2000 anti-actin	1:5000 anti-mouse HRP
1:250 anti-transferrin	1:5000 anti-mouse HRP
1:6000 anti-caveolin	1:10,000 anti-rabbit HRP
1:2000 anti-ERK1/2	1:2000 anti-rabbit HRP
1:500 anti-tubulin	1:5000 anti-mouse HRP
1:500 anti-EEA1	1:500 anti-goat HRP

Membranes were washed and incubated in SuperSignal West Pico chemiluminescent substrate. Protein bands were visualized on a Kodak Image Station 440 and quantified using Kodak 1D software.

Data and Statistical Analysis

Graphs and statistical calculations were done using GraphPad Prism 4 software (San Diego, CA). Data points are represented as the mean of three or more independent experiments ± standard error and compared for statistical significance using unpaired, two-tailed Student's t-tests or 1-way ANOVA with Bonferroni's post-hoc test unless otherwise stated. Significance was set at $p < 0.05$. Maximal [^{35}S]GTPγS stimulation and EC_{50} values were calculated from individual concentration-effect curves using fixed slope sigmoidal dose-response curve fit analysis in GraphPad Prism. To calculate half-life for time-course decay of overshoot experiments, data was fitted to a one-site exponential decay model, with standard error calculated from two or more independent experiments.

Results

Effects of cholesterol depletion and addition on AC sensitization in C6μ cells

Cholesterol depletion and MβCD

Sensitization refers to the increased enzymatic activity of AC caused by chronic treatment with an agonist to an inhibitory G protein-coupled receptor, such as an opioid agonist. AC sensitization is expressed as an overshoot in cAMP produced after removal of the inhibitory agonist and heterologous stimulation of AC. In order to determine the effect of cholesterol depletion on AC sensitization in C6μ cells, we used the cholesterol-sequestering agent methyl-β-cyclodextrin (MβCD). We first had to evaluate the minimum concentration of MβCD that could cause a selective change in AC overshoot while keeping acute AC inhibition constant. Many earlier studies involving lipid rafts utilized >10 mM MβCD to elicit significant cholesterol depletion, however, these studies either used isolated detergent-resistant membranes or did not test long-term functionality of cells (17,19,20). Therefore, we wanted to use a lower concentration of MβCD to retain cell viability while testing the effect of cholesterol depletion on chronic mu opioid signaling. Trypan blue exclusion experiments demonstrated that incubation of C6μ cells in 4 mM MβCD for up to 1 h has no effect on cell viability (Figure 3A).

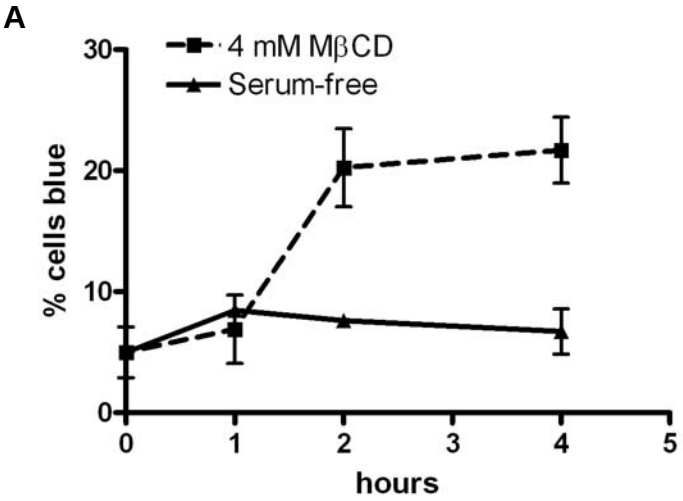

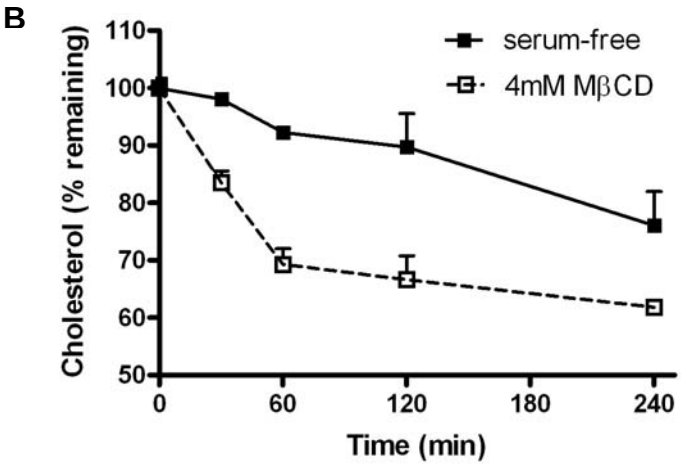

Figure 3. MβCD treatment for 1 hr achieves maximal cholesterol depletion without affecting cell viability. *A*, cells treated with serum-free DMEM or 4 mM MβCD for 0-4 h were counted in a hemocytometer after incubation in Trypan blue. Dead cells were stained blue while viable cells remained colorless. Data are presented as the mean % of total cells stained blue ± S.E.M (n=1, in duplicate). *B*, total cholesterol in the cells was measured after treatment with serum-free DMEM or 4 mM MβCD for 0-4 hr. Data is presented as the mean % of total cellular cholesterol remaining ± S.E.M (n=3, in duplicate).

However, longer treatment times did increase cell death (Figure 3A). Furthermore, maximal separation of cholesterol depletion was reached after 1 h incubation in 4 mM MβCD (69.28 ± 2.76% of original cholesterol remaining) (Figure 3B). At later time points, cholesterol in MβCD-treated and serum-free control cells both declined at similar rates (Figure 3B). Therefore, we studied the effect of cholesterol removal by 4 mM MβCD for 1 h on AC sensitization caused by the mu opioid agonist DAMGO (Figure 4).

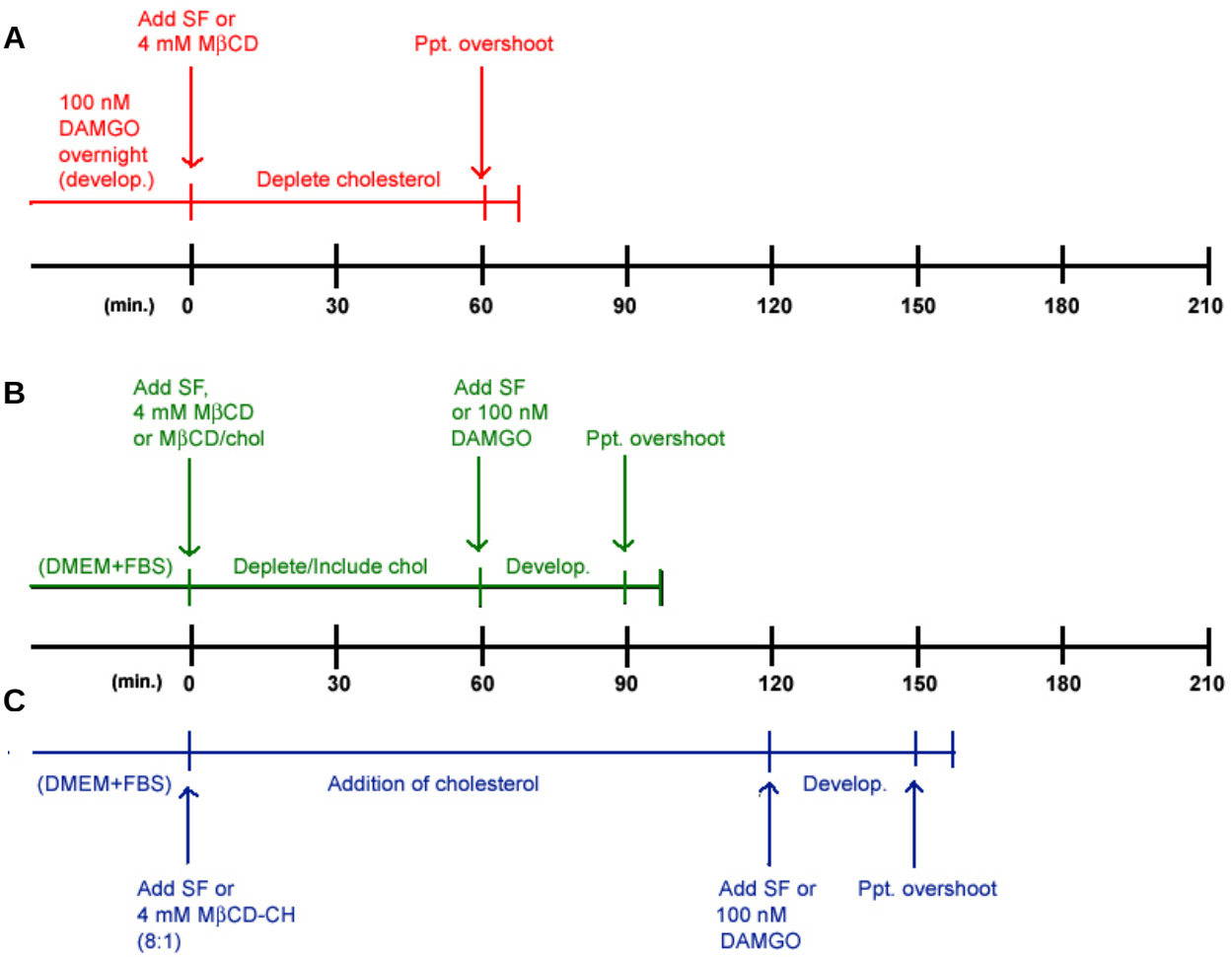

Figure 4. Diagram of methods used to modulate cellular cholesterol levels and investigate the effect on the development and expression of adenylyl cyclase sensitization. In all experiments, overshoot was precipitated by 10 μM naloxone, 5 μM forskolin and 1 mM IBMX for 10 min. In acute AC inhibition experiments (not shown), the naloxone was replaced by 10 nM DAMGO (mu-opioid agonist). *A*, cells were treated with 100 nM DAMGO overnight in DMEM + FBS media to sensitize AC. The media was then replaced with either serum-free DMEM or 4 mM MβCD (deplete cholesterol) for 1 h, followed by precipitation of overshoot. *B,* either serum-free DMEM, 4 mM MβCD (deplete cholesterol) or MβCD/cholesterol suspension (include cholesterol) was added to cells for 1 h. AC was sensitized using chronic (30 min) 100 nM DAMGO treatment, followed by precipitation of overshoot. *C,* cells were treated with serum-free DMEM or MβCD-CH complex (addition of cholesterol) for 2 h. AC was sensitized using chronic (30 min) 100 nM DAMGO treatment, followed by precipitation of overshoot.

Effect on AC overshoot

Cells were first treated with serum-free DMEM, 4 mM MβCD, or MβCD/cholesterol suspension for 1 hr (Figure 4B). The media was changed and cells were incubated at 37°C in 100 nM DAMGO for 30 min to sensitize AC. Overshoot was precipitated by the addition of the opioid antagonist naloxone and stimulation of AC by forskolin. The results show that overshoot is significantly reduced from 294.75 ± 32.22% of forskolin-stimulated cAMP accumulation in serum-free controls to 198.28 ± 14.01% by pre-treatment with MβCD (Figure 5).

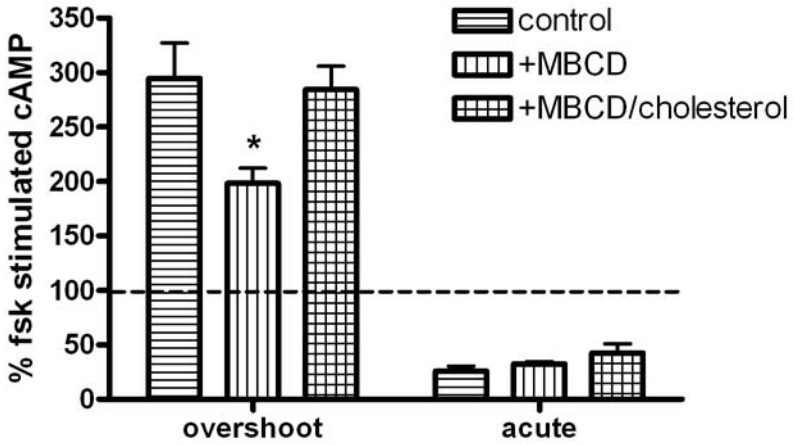

Figure 5. Cholesterol depletion using MβCD affects the development of overshoot, but has no significant effect on short-term inhibition. C6μ cells were pre-treated with 4 mM MβCD, MβCD/cholesterol suspension or serum-free DMEM for 1 hr prior to chronic (30 min) treatment with 100 nM DAMGO. Overshoot was precipitated with naloxone in the presence of 5 μM forskolin as described in "Materials and Methods." 10 nM DAMGO was used for acute inhibition of adenylyl cyclase. Data presented as the mean % of forskolin-stimulated cAMP accumulation ± S.E.M ($n \geq 3$, in duplicate). Forskolin-stimulated cAMP accumulation (forskolin only) is indicated by the dashed line. *$p < 0.05$ compared with control using one-way ANOVA with Bonferroni's post-hoc test. Acute inhibition by DAMGO was similar in all treatments ($p > 0.05$) by one-way ANOVA with Bonferroni's post-hoc test.

Inclusion of cholesterol in the media with MβCD, prepared as described in "Materials and Methods", prevented the effect of MβCD. Acute inhibition by 10 nM DAMGO (mu-opioid agonist) was not affected by either the addition of MβCD or the MβCD/cholesterol. To determine if addition of excess cholesterol to C6μ cells would affect overshoot, cells were

incubated in MβCD-CH for 2 h prior to chronic DAMGO treatment (100 nM DAMGO, 30 min) (Figure 4C). Despite the increase in cellular cholesterol from 18.9 ± 1.6 mg cholesterol/mg protein to 31.0 ± 1.5 mg/mg after 2 h, no significant difference in overshoot was observed (Figure 6).

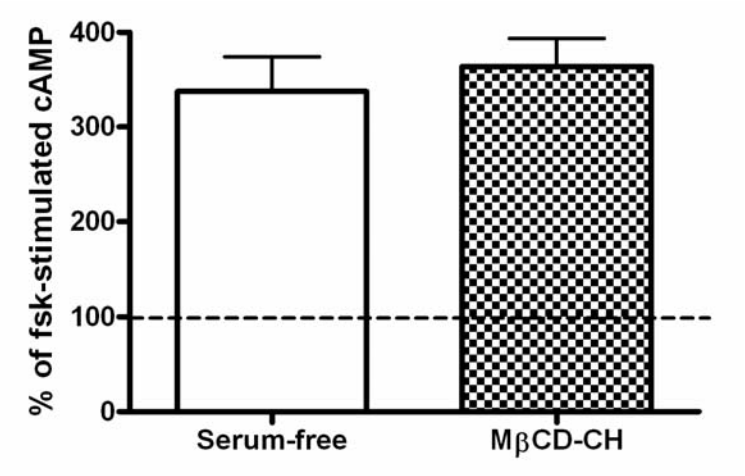

Figure 6. Addition of cholesterol prior to development of adenylyl cyclase overshoot has no effect. Cells were incubated in a 4 mM MβCD-cholesterol complex (MβCD-CH) or serum-free media for 2 h prior to development of overshoot using chronic (30 min) 100 nM DAMGO treatment, as described in "Materials and Methods." Data presented as the mean % forskolin-stimulated cAMP accumation ± S.E.M. ($n \geq 2$, in duplicate). Forskolin cAMP accumulation is indicated by the dashed line. Addition of cholesterol did not significantly change forskolin-stimulated adenylyl cyclase overshoot by unpaired, two-tailed Student's t-test.

Mechanism of effect

The objective of these studies was to investigate the mechanism of the decrease in overshoot by MβCD. Our hypothesis was that cholesterol depletion will affect the development phase of overshoot but not the expression phase. To measure the effect of cholesterol depletion on the expression of overshoot, we treated cells with 100 nM DAMGO overnight in regular media to allow sensitization to develop normally (Figure 4A). We then treated the cells with 4 mM MβCD or serum-free DMEM for 0-4 h and measured the overshoot after this incubation by precipitating withdrawal with naloxone and forskolin as described above. Both serum-free and 4

mM MβCD-treated cells had equal rates of decay of overshoot, measured as the half-life of decay of cAMP accumulation over time [serum-free: ($t_{1/2}$ = 59.52 ± 19.58 min), MβCD: ($t_{1/2}$ = 64.28 ± 6.28), $p < 0.05$] (Figure 7).

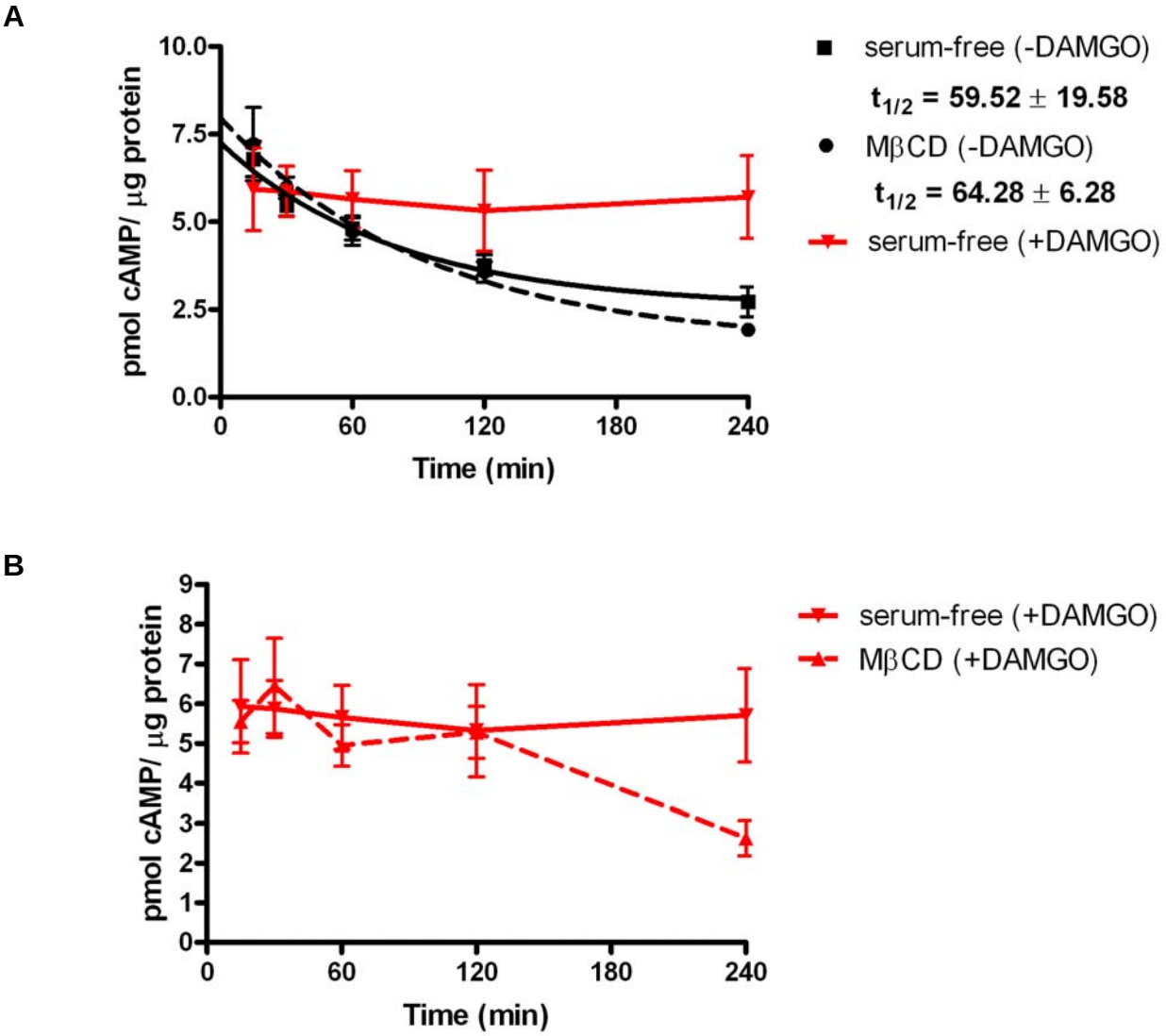

Figure 7. Decay of adenylyl cyclase overshoot is similar during incubation in serum-free media or MβCD, and is prevented by the addition of DAMGO to the media. *A*, adenylyl cyclase overshoot after cells were incubated in serum-free media, serum-free with 100 nM DAMGO or 4 mM MβCD for 0-4 h following chronic (24 h) 100 nM DAMGO treatment. Data presented as pmol cAMP accumulation per µg protein ± S.E.M. ($n \geq 3$, in duplicate). The zero time-point is omitted because of the effect of FBS removal on adenylyl cyclase activity, as explained in "Results." Rates of decay were measured using a one-site exponential decay model [serum-free: ($t_{1/2}$ = 59.52 ± 19.58 min), MβCD: ($t_{1/2}$ = 64.28 ± 6.28)] and were not significantly different by unpaired, two-tailed Student's t-test. MβCD treatment along the entire time-course

was not significant by two-way ANOVA [treatment: F(1, 44) = 0.01352, p = 0.9080] and the decrease in overshoot by MβCD at each time point was not significant by Bonferroni's post-hoc test. *B*, maintenance of overshoot by addition of DAMGO to either serum-free or 4 mM MβCD for 0-4 h. Data presented as pmol cAMP accumulation per μg protein ± S.E.M. (n ≥ 3, in duplicate).

MβCD treatment on the entire time-course was not significantly different by 2-way ANOVA [treatment: F(1, 44) = 0.01352, p = 0.9080] and the decrease by MβCD at each time point was not significant by Bonferroni's post-hoc test. This decay in overshoot was prevented, as expected, by the addition of 100 nM DAMGO in the serum-free treatment throughout the entire time-course (Figure 7). However, the addition of DAMGO in the MβCD was only able to maintain overshoot up to 2 hrs, after which cAMP accumulation dropped sharply (Figure 7B). This may be due to decreased viability of cells after long-term exposure to MβCD, as described previously (Figure 3A).

Although there was no effect of cholesterol depletion by MβCD on the overshoot developed by overnight DAMGO treatment, we did see a decrease in overshoot developed by only 1 h DAMGO when cells were treated with MβCD for 1 h between the development and precipitation of overshoot (Figure 8).

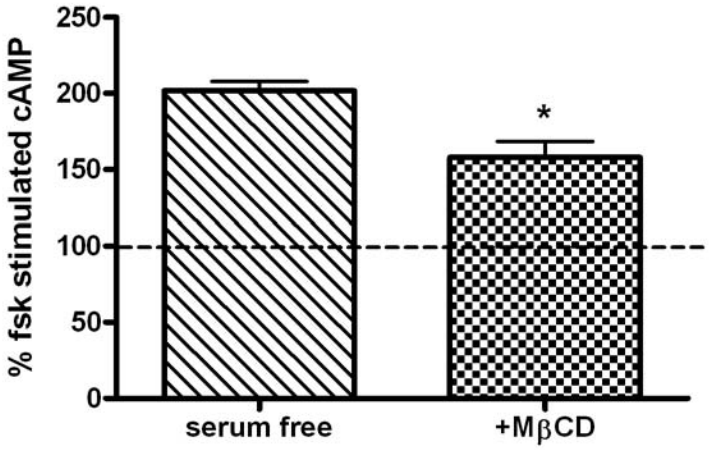

Figure 8. Effect of MβCD on adenylyl cyclase overshoot after 1 hr chronic agonist treatment. Cells were treated with either serum-free or 4 mM MβCD after sensitization of adenylyl cyclase with chronic (1 h) 100 nM DAMGO treatment. Data is presented as the mean % forskolin-stimulated cAMP accumation compared with basal ± S.E.M. (n = 3, in duplicate). Forskolin cAMP accumulation is indicated by the dashed line. *p < 0.05 by unpaired, two-tailed Student's t-test.

These different findings suggest that there may exist different mechanisms of sensitization, depending on the duration of agonist exposure, such as increased protein expression.

Importance of fetal bovine serum

Fetal bovine serum (FBS) also seemed to have an effect on cellular cholesterol and overshoot. In the time-trial cholesterol depletion with 4 mM MβCD, we observed that removal of FBS from the cell culture media caused a slight decrease in cellular cholesterol over time, though less than the decrease induced by MβCD (Figure 5B). Also, we observed a sharp decrease in cAMP accumulation from the 0 to 15 min time point that immediately leveled off in subsequent time points (Figure 9).

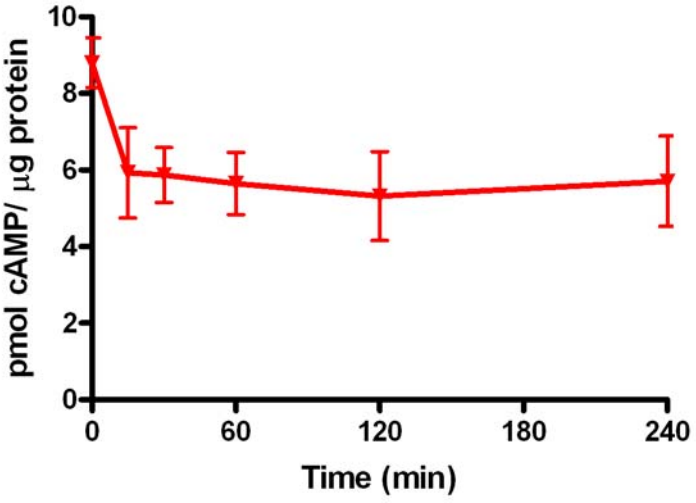

Figure 9. Removal of FBS decreases adenylyl cyclase overshoot for up to 15 min. Cells were incubated in serum-free media with 100 nM DAMGO following chronic (24 h) 100 nM DAMGO treatment in DMEM + 10% FBS. Data is presented as the mean pmol cAMP accumulation per µg protein ± S.E.M. (n = 4, in duplicate).

These findings suggest that components in FBS have the ability to sensitize AC, which rapidly diminishes within 15 min of its removal from the cell medium. Clark et al. also observed this effect and hypothesized that C6 cells may have a tonic level of sensitization, maintained by a component in FBS, that is made apparent by the removal of FBS (21).

Separation of lipid raft and non-raft fractions

Initial modifications to the original raft separation protocol

Because of the importance of cholesterol in sensitization, our next step was to identify mu-opioid receptor signaling elements in lipid rafts, which are membrane microdomains enriched in cholesterol and involved in G protein signaling. To obtain functional raft and non-raft membrane fractions, we modified a detergent-free raft preparation method by Smart et al. (15). Briefly, C6μ cells were grown to confluence in DMEM with 10% FBS. Cells were scraped into a calcium-free lifting buffer and spun at 1400 x g for 5 min. The pellet was resuspended in buffer A (0.25 M sucrose, 1 mM EDTA, 20 mM Tricine, pH 7.8, protease inhibitor) containing 10 mg/mL BSA to maintain AC function, homogenized using a Dounce homogenizer and spun at 1000 x g for 10 min. The postnuclear supernatant (PNS) was collected and the pellet was homogenized and centrifuged again at the same conditions. Both supernatants were combined, layered on top of 30% Percoll and spun at 84,000 x g for 30 min. The plasma membrane band (PM) was extracted, mixed with buffer A and sonicated. The PM fraction was mixed with Optiprep for a final concentration of 23% (w/v) at the bottom of an ultracentrifuge tube, with a 20-10% Optiprep gradient layered on top and spun at 52,000 x g for 90 min. The top 5 mL was collected, mixed with 50% Optiprep added to the bottom of another tube, 5% Optiprep was

layered on top and the tube spun at 52,000 x g for 90 min. The raft membrane band was collected at the 5% Optiprep interface.

Membrane fractions prepared using this slightly modified protocol had low protein concentration as measured by Bradford protein assay (22), limiting the number of subsequent experiments on the fractions. Measurement of G protein activation using [^{35}S]GTPγS binding assays showed that membrane fractions had functionality after stimulation by the selective mu-opioid agonist DAMGO (Figure 10).

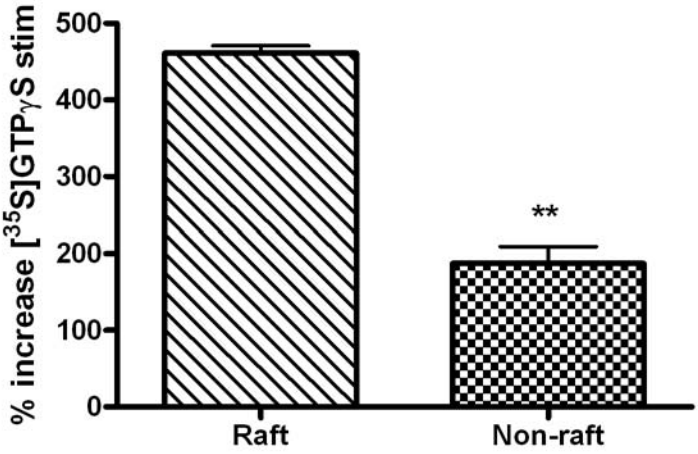

Figure 10. Lipid raft and non-raft fractions have different levels of G protein activation. [^{35}S]GTPγS binding in raft and non-raft membranes isolated using the original protocol by Smart et al. (15) was evaluated as described in "Materials and Methods." Data expressed as the mean % increase in [^{35}S]GTPγS stimulation compared with basal ± S.E.M. (n=1, in duplicate). **$p < 0.01$ by unpaired, two-tailed Student's t-test. Basal values: (Raft: 3.25 ± 0.22 fmol bound/mg protein, Non-raft: 0.34 ± 0.01 fmol/mg).

Basal G protein activation was higher in raft fractions (3.25 ± 0.22 fmol bound/mg protein) compared with non-raft fractions (0.34 ± 0.01 fmol/mg), indicating an enrichment of G proteins in raft fractions. The ability of the mu opioid agonist DAMGO to stimulate [^{35}S]GTPγS binding was also higher in raft fractions compared to non-raft fractions (Figure 10). This may be due an increase in mu-opioid receptor concentration levels in raft fractions as described later

(Figure 18C). These results verify that the opioid signaling pathways remain functional in fractions isolated using this method.

Purity of raft and non-raft fractions

We next evaluated the purity of the preparation and attempted to modify to protocol to enhance purity and yield. Purity of raft and non-raft fractions were evaluated based on two protein markers: transferrin, a non-raft marker and caveolin, a raft-associated protein (23). Western blots showed that while caveolin was higher in raft fractions, so was the amount of transferrin receptor. One hypothesis to explain this result was that the sonication step was not sufficient to disrupt raft and non-raft domains prior to separation in the Optiprep gradient. Increasing the amount of sonication, however, decreased the ratio of caveolin to transferrin in the raft fraction (Figure 11A).

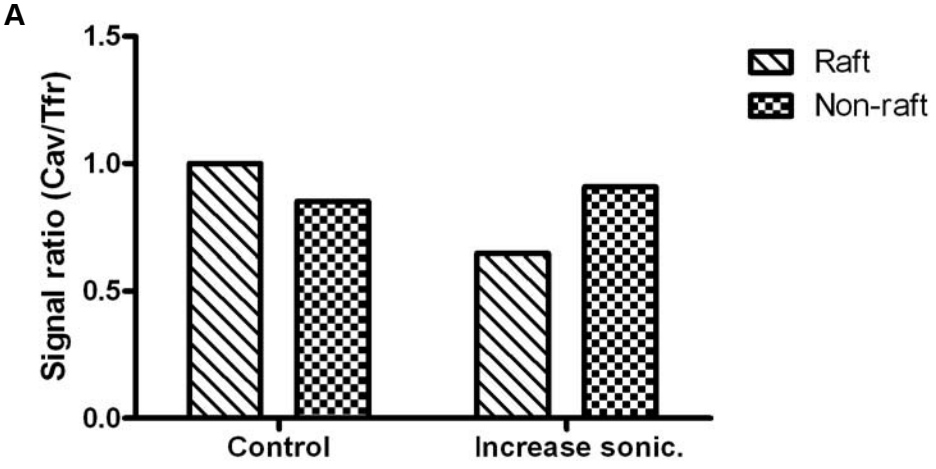

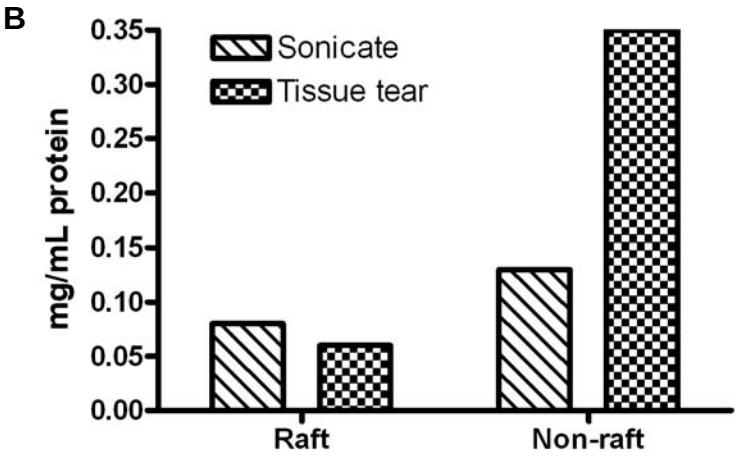

Figure 11. Increasing sonication of plasma membranes decreases the separation of lipid raft and non-raft membranes while tissue tearing increases protein concentration in non-raft membranes. *A,* the amount of sonication of plasma membranes prior to separation of lipid raft and non-raft components in Optiprep was increased. Transferrin receptor (Tfr) and caveolin (Cav) protein levels were evaluated by Western blotting as described in "Materials and Methods." *B*, sonication of the plasma membrane fraction prior to separation of raft and non-raft components was substituted with tissue tearing as described in "Results."

Also, we substituted sonication of the plasma membrane band (12 pulses at 2.2, 1 sec each) with tissue tearing (level 3, 15 sec), which increased protein concentration of the non-raft fraction and slightly decreased the protein concentration of the raft fraction (Figure 11B). We decided to switch from sonication to tissue tearing not only because of this improvement, but also because we thought that this method was faster and more reliable. In addition, Western blots showed that raft fractions had higher caveolin than non-raft fractions after tissue tearing. Replicate experiments, however, also showed that transferrin was higher in raft fractions, and indicated a lack of separation (data not shown).

The mitochondrial protein prohibitin was used as a non-plasma membrane marker to evaluate the purity of plasma membrane fractions. In order to improve the purity of the plasma membrane separation, we revised the protocol to include a centrifugation step prior to plasma membrane separation in 30% Percoll. Bovine serum albumin and protease inhibitors were also eliminated from buffer A in order to prevent skewing of protein assay results. After harvesting

and pelleting cells as in the original protocol, postnuclear supernatants were combined in a tube and centrifuged at 9000 rpm (9500 x g) in a Beckman JA-20 rotor for 10 min, following a protocol described by Rego et al. (24). A large brown pellet (mitochondria) at the bottom of the tube was observed and was resuspended in 0.5 mL 50 mM Tris buffer. Western blots showed that prohibitin was present in the mitochondrial pellet and in higher amounts per mg protein than in the plasma membrane fraction (data not shown). Experiments to determine receptor number were also begun at this point, and showed that mu-opioid receptor concentration increased (from 1.862 to 2.866 pmol receptor/mg protein) during the plasma membrane purification step. However, protein concentrations (as measured by BCA from this point forward) for raft and non-raft fractions continued to be relatively low at <0.02 mg/mL and 0.13 mg/mL, respectively. Therefore, in subsequent preparations, this pelleting step was skipped in order to increase protein yields and because mitochondrial contamination of the plasma membranes was relatively low.

Addition of a sucrose-HEPES buffer

Prpic et al. reported that using this sucrose-HEPES buffer for plasma membrane isolation increased the protein yield, improved membrane protein activity and decreased mitochondrial contamination when compared with using a regular sucrose buffer (25,26). As a result, we decided to change buffer B from the one used by Smart et al. (0.25 mM sucrose, 6 mM EDTA, 120 mM Tricine, pH 7.8) to a sucrose buffer containing HEPES and EGTA. In addition, after harvesting and pelleting the cells at 1600 rpm for 3 min, the pellet was resuspended and homogenized in buffer B to attain a cell concentration of 6% (w/v) instead of resuspending in a fixed 1 mL of buffer B. The homogenate was then added to Percoll and centrifuged to separate plasma membranes. In our experiments, use of sucrose-HEPES (buffer B) instead of the original

buffer A in the modified raft separation protocol significantly increased the protein concentration in the non-raft fraction ($p < 0.05$) with no change in the raft fraction (Figure 12A).

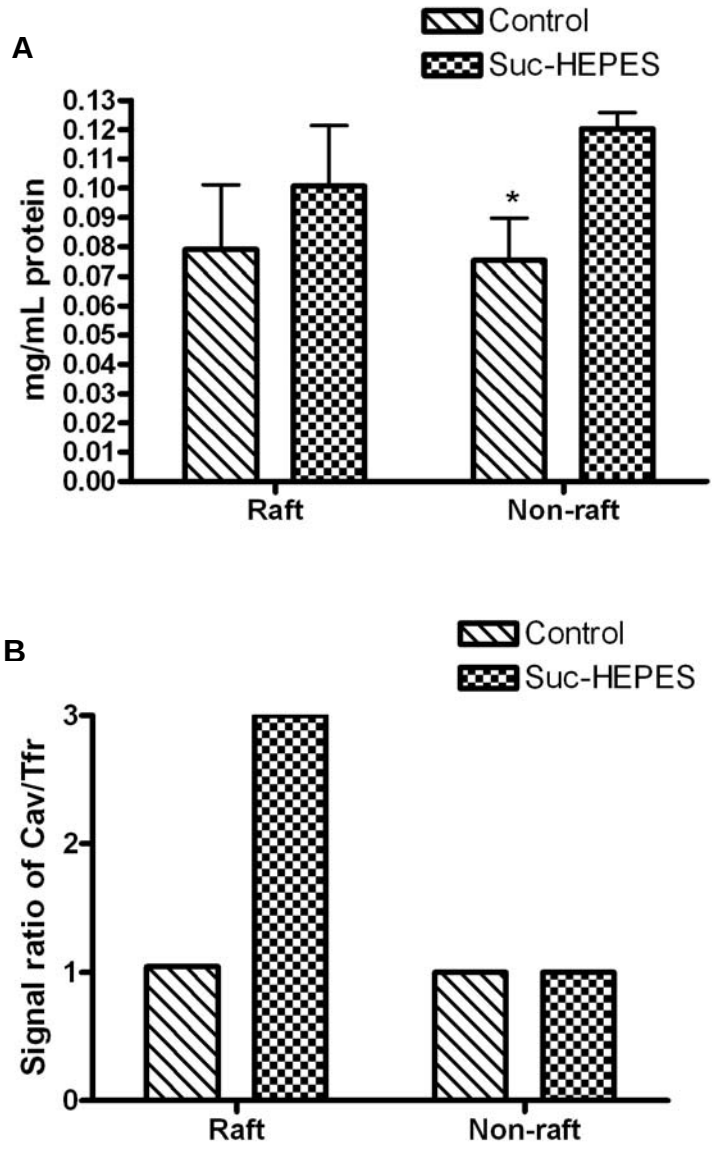

Figure 12. Sucrose-HEPES buffer increases protein concentration in non-raft fractions and separation of lipid raft and non-raft membranes. Instead of using the buffer A (control) described in the protocol by Smart et al. (15), cells were resuspended and homogenized in a sucrose-HEPES buffer (buffer B) described by Prpic et al. (25). *A*, protein concentrations were measured by BCA assay as described in "Materials and Methods." Data presented as the mean mg protein per mL ± S.E.M. *$p < 0.05$ by unpaired, two-tailed Student's t-test. *B*, transferrin (Tfr) and caveolin (Cav) protein levels were measured by Western blotting as described in "Materials and Methods."

The change also led to increased separation of raft and non-raft fractions, as shown by the 3-fold increase in the ratio of caveolin to transferrin in raft fractions isolated using buffer B (Figure 12B).

Reduction in preparation time

Because the original protocol required several ultracentrifugation steps and over 6 hours to complete, one of our objectives was to reduce the number of steps to increase functionality by the replacing the continuous Optiprep gradient with a single discontinuous gradient spin. Plasma membranes isolated from the Percoll spin step were mixed with 50% Optiprep to attain a final concentration of 23% (w/v). The mixture was placed at the bottom of an ultracentrifuge tube and instead of using 5 mL of a 20%-10% continuous Optiprep gradient, we layered 2.5 mL of 15% and 2.5 mL of 5% Optiprep on top. The concentrations of Optiprep were determined by observing the locations of membrane bands in the original protocol: non-raft fractions were located 2/3 from the bottom of the tube in the 20-15% gradient after the first Optiprep spin step and raft fractions were located at the interface between ~15% and 5% Optiprep after the second Optiprep spin step. Bands were observed at the 15/5% interface (raft) and at the 23/15% interface (non-raft). Fractions were also taken from areas above, below and between the bands. Fractions isolated using this method had equal or higher protein concentrations than the previously-used method, and had a higher level of cholesterol enrichment when comparing the raft to non-raft fractions (Figure 13).

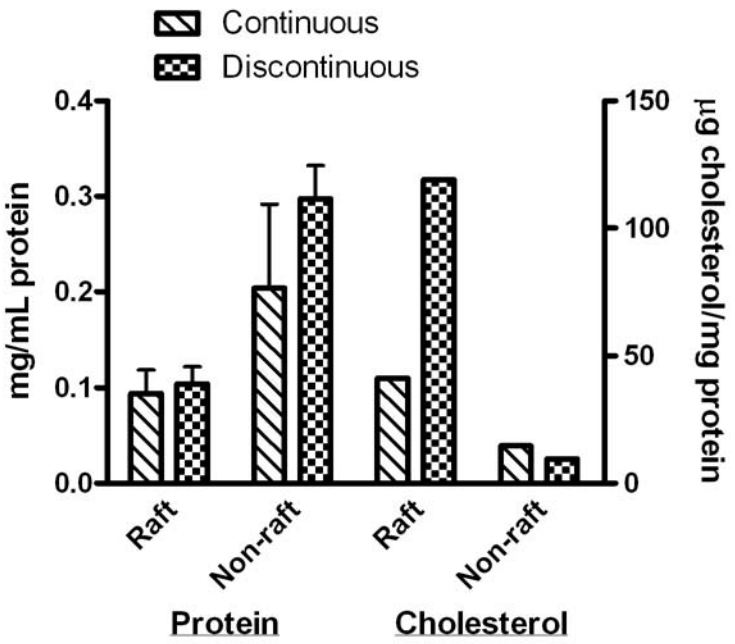

Figure 13. Use of a discontinuous Optiprep gradient has no effect protein concentration, but increases cholesterol concentration in isolated raft membranes. Instead of using a 20-10% continuous Optiprep gradient as described in the protocol by Smart et al. (15), a 15/5% discontinuous Optiprep gradient was used for separation of raft and non-raft membranes, as described in "Results." Protein concentration results are presented as the mean mg protein/mL ± S.E.M. ($n \geq 2$).

Optiprep concentration of isolated fractions

Although cholesterol enrichment in raft fractions was demonstrated, total protein yields in raft fractions remained low. To concentrate protein in the raft and non-raft fractions, after separation in the discontinuous Optiprep gradient, everything at and above the upper interface was taken as the raft fraction (~5% Optiprep) and everything below the interface (~19% Optiprep) was taken as the non-raft fraction. Both fractions were diluted to ~4% Optiprep in TES buffer B and spun at 22,000 rpm for 90 min in a Beckman Ti 70.1 rotor. While a pellet was observed raft fraction, a more diffuse aggregate was observed in the non-raft fraction, possibly because the concentration of Optiprep was too high. As a result, we decreased the concentrations of Optiprep used for the discontinuous gradient to 12% and 2% (full gradient = 23/12/2 %

Optiprep). Similar to the previous gradient, a cloudy band was observed at the 12/2 % Optiprep interface. The "raft" fraction was taken from above and including this band and the "non-raft" fraction was taken from below this band. Both fractions were diluted to ~1% Optiprep in TES buffer B and spun at 22,000 rpm for 90 min in a Beckman Ti 70.1 rotor. The resulting pellets were resuspended in a small volume of TES buffer and had a higher protein concentration than previous experiments (Figure 14A).

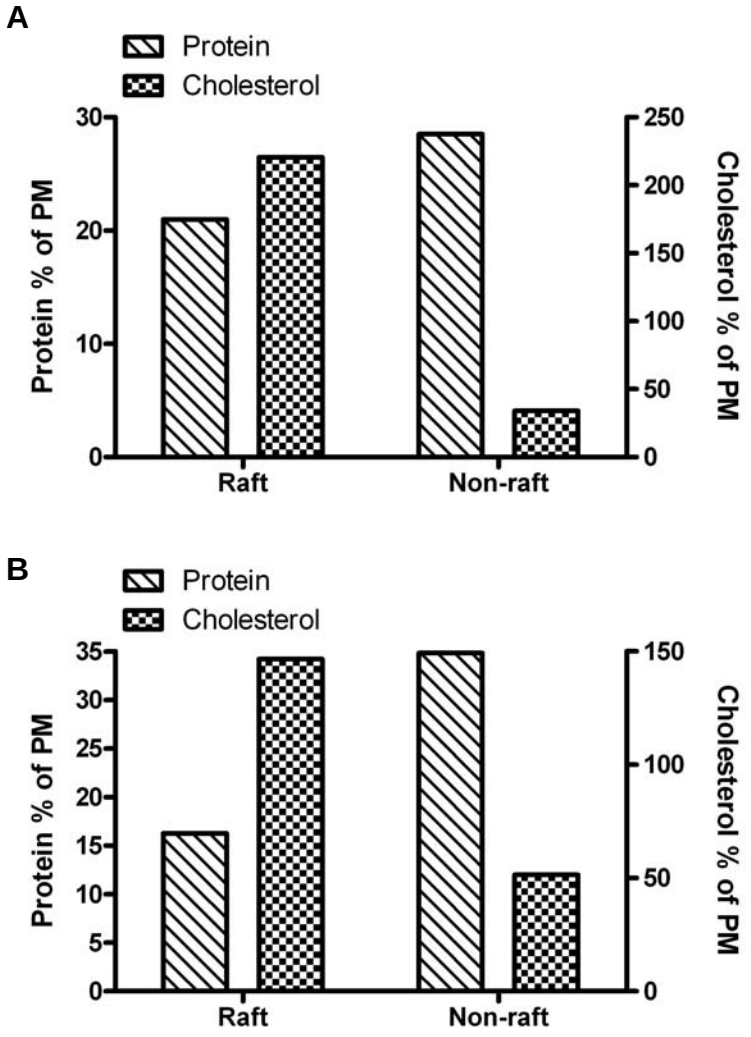

Figure 14. Summary of raft and non-raft concentrating modifications. All modifications are described in "Results." *A,* separation of raft and non-raft fractions was done using a 12/2% Optiprep gradient. Fractions were diluted with TES buffer and pelleted. *B,* the 12/2% Optiprep gradient was reduced to a single 12% Optiprep layer (floating fraction).

To increase protein concentration, we eliminated the 2% layer and extracted the raft band and everything above it, since the band had moved slightly further into the 12% layer. We kept this modification in the final protocol because it saved a significant amount of time (90 min), even if cholesterol concentrations were slightly decreased as a result (Figure 14B).

Final protocol

From these slight modifications, we devised a protocol to use with consistency to try to obtain functional raft and non-raft membranes. This protocol is described in detail in "Materials and Methods" (Figure 15).

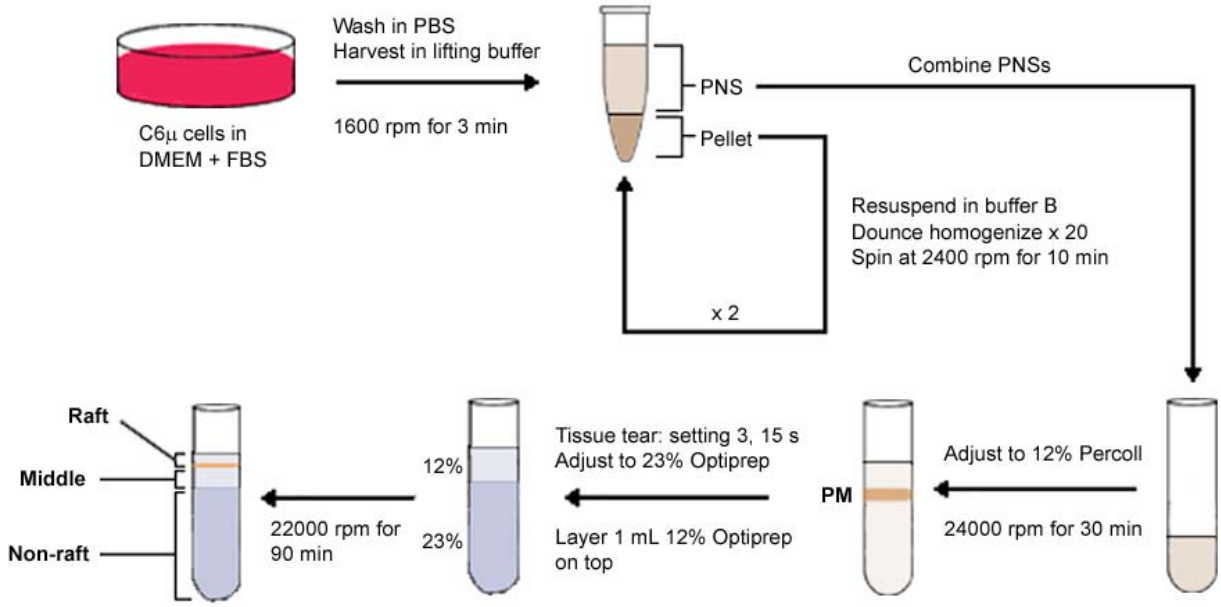

Figure 15. **Diagram of the final raft separation protocol**. The final raft separation protocol is based on the original protocol by Smart et al. (15) and is described in "Materials and Methods."

Briefly, C6μ cells were harvested in lifting buffer, resuspended in buffer B and homogenized in a Dounce homogenizer before centrifugation at 2400 rpm for 10 min. The postnuclear supernatants (PNS) were removed, adjusted to 12% (w/v) Percoll and centrifuged at 24000 rpm for 30 min to separate the plasma membranes (PM). A Tissue Tearor was used to disrupt crude PM into fragments. The membrane mixture was adjusted to 23% (w/v) Optiprep and 12% (w/v) Optiprep was layered on top before centrifugation at 22000 rpm for 90 min. A cloudy band appeared near the top of the tube and three fractions were collected: one from above and including the top band ("raft"), one from between the top and bottom bands ("middle"), and one from everything below and including the bottom band ("non-raft"). Three bands were taken instead of just the raft and non-raft bands in order to better evaluate the degree of separation

across the Optiprep gradient. By shortening the protocol, we were able to reduce the number of steps where membrane components would be lost during processing or transfer to another tube. We also significantly decreased the overall time from start to completion from 6 hours to 4 hours.

Identification of transferrin and caveolin protein markers in raft or non-raft fractions was performed by Western blotting. Additional protein markers were also used to characterize the isolated fractions. Cytoskeletal elements are thought to be associated with lipid rafts and have a role in facilitating membrane receptor signaling processes (5). Head et al. showed that disruption of the cytoskeleton in cardiac myocytes with either colchicine (to disrupt tubulin) or cytochalasin D (to disrupt actin) led to the exclusion of caveolin and AC 5/6 from lipid raft fractions (27). Actin is also thought to play a role in the clustering of raft proteins and stabilization of raft microdomains (28). As a result, we used tubulin and actin as possible lipid raft markers. Another protein marker that we tested was EEA1, an endosomal marker that was shown to be associated with internalized detergent-resistant membranes containing caveolin (29,30). This is not always the case, however: another study with MCF-7 cells showed that internalized endosomes containing EEA1 did not contain caveolin (31). We also tested for ERK, a mitogen-activated protein kinase (MAP kinase) that has been shown to co-localize with caveolin along with several other components of the MAP kinase signaling pathway (32,33). Both studies use the raft separation method of Smart et al. (15) and also show that stimulation of isolated raft fractions containing platelet-derived growth factor (PDGF) can activate MAP kinases and phosphorylation of tyrosine (32,33).

Western blots showed that ratios of non-raft marker transferrin versus raft marker caveolin were similar across all fractions, indicating a lack of separation between raft and non-raft membranes (Figure 16B).

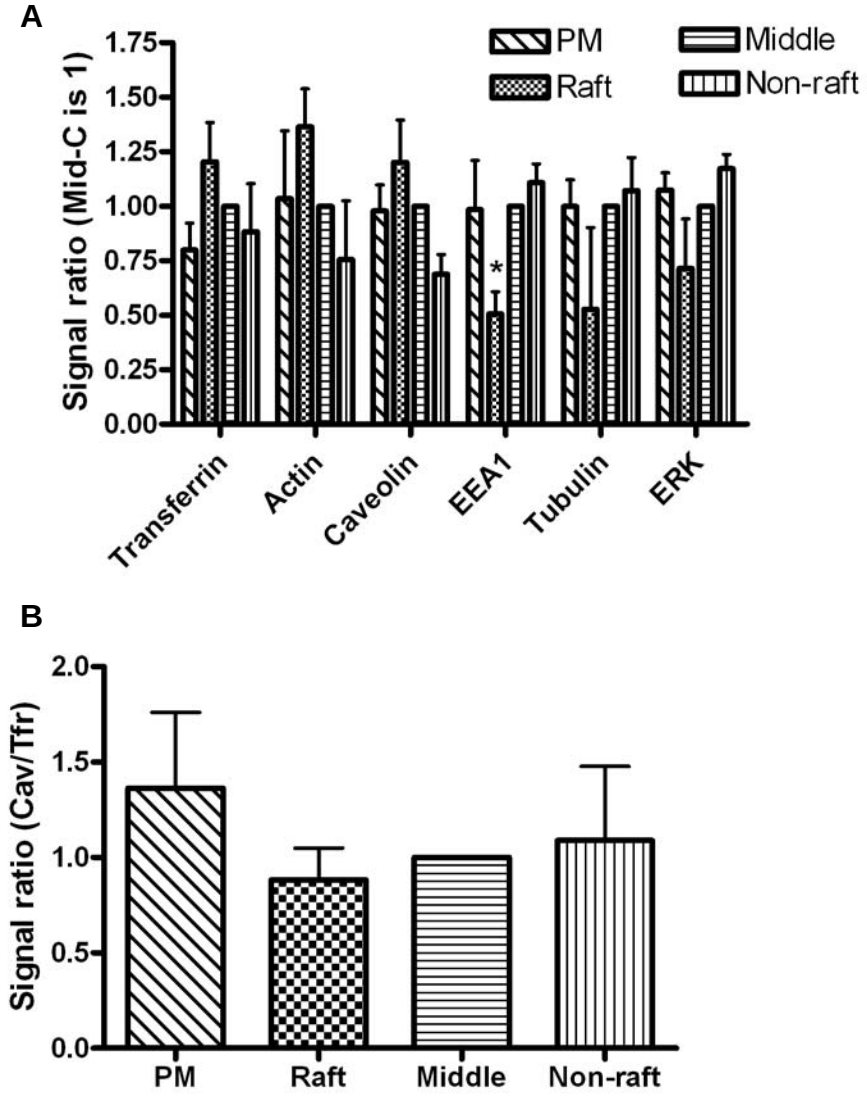

Figure 16. Protein marker levels are similar across all fractions isolated using the modified separation protocol with the exception of EEA1. Fractions were isolated using the modified detergent-free raft separation protocol described in "Materials and Methods." *A,* protein marker levels for transferrin receptor, actin, caveolin, EEA1, tubulin and ERK were determined by Western blotting as described in "Materials and Methods." Protein levels are expressed as the ratio of signal net intensity when compared with the corresponding protein signal in the middle fraction. *B,* signal net intensity ratio of caveolin to transferrin receptor in each fraction was also calculated. Data is presented as the mean ratio of signal net intensity ± S.E.M. ($n \geq 3$). *$p < 0.05$ by one-way ANOVA with Bonferroni's post-hoc test (within the "EEA1" group).

There were similar results with other protein markers, with the exception of EEA1, which was lower in the raft fraction compared with the PM and bottom fractions (Figure 16A). While

the trend was not statistically significant by one-way ANOVA and Bonferroni's post-hoc test ($p = 0.0668$), it does show that raft microdomains may have limited interaction with endosomes compared with non-raft domains. One study showed that TGF-β receptors in lipid raft and non-raft domains internalize into different endocytic compartments, with raft receptors localizing with caveolin and non-raft receptors localizing with EEA1 (34).

Fractions isolated using the final raft preparation protocol showed a significant increase in percent recovery of cholesterol ($p < 0.05$) and mu-opioid receptor ($p < 0.05$) compared with previous versions of the protocol (Figure 17).

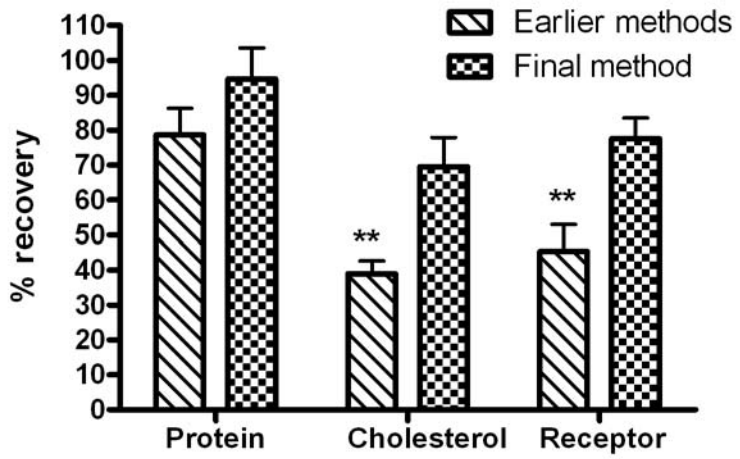

Figure 17. **Recoveries of protein, cholesterol and receptor are improved using the modified separation protocol.** Protein, cholesterol and receptor quantities were measured in fractions isolated using the modified detergent-free raft separation protocol (final) described in "Materials and Methods" and earlier modifications of the original protocol by Smart et al. (15). Recoveries were calculated as the % of total protein, cholesterol or receptor in raft, middle and non-raft fractions when compared with the plasma membrane fraction. Data is presented as the mean % recovery ± S.E.M. ($n \geq 5$). **$p < 0.01$ by unpaired, two-tailed Student's t-test.

While protein concentrations in the three Optiprep fractions were significantly lower than the PM fraction, they are still higher than the concentrations reported by Smart et al. [~0.25 mg/mL (vs. 1.36 ± 0.174 mg/mL) for the PM fraction and ~0.04 mg/mL (vs. 0.241 ± 0.061 mg/mL) for the raft fraction] (Figure 18A).

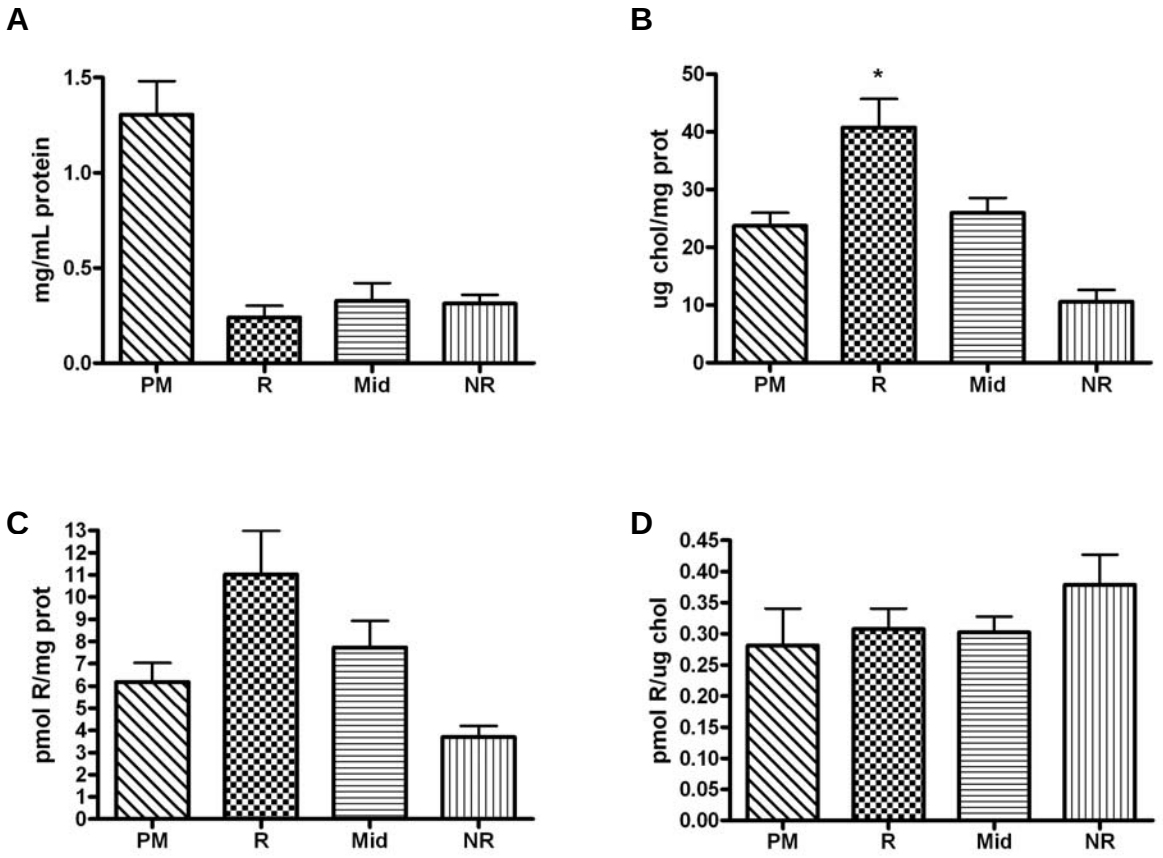

Figure 18. Summary of protein, cholesterol and receptor concentrations in fractions isolated using the modified separation protocol. *A,* mean mg protein per mL ± S.E.M. (n = 5). *B,* mean μg cholesterol per mg protein ± S.E.M. (n = 4). *p < 0.05 by one-way ANOVA with Bonferroni's post-hoc test. *C,* mean pmol receptor per mg protein ± S.E.M. (n = 5). Differences in receptor per protein is non-significant across fractions by one-way ANOVA with Bonferroni's post-hoc test, though a trend is observed (p = 0.0860). *D*, mean pmol receptor per μg cholesterol ± S.E.M. (n = 4). Values of receptor per cholesterol are similar across fractions (p > 0.05) by one-way ANOVA with Bonferroni's post-hoc test.

Cholesterol per protein measurements in the raft fraction (40.76 ± 4.96 ug/mg) were also significantly higher than both the PM (23.73 ± 2.26 ug/mg) and middle (25.99 ± 2.56 ug/mg) fractions by one-way ANOVA and Bonferroni's post-hoc test (p < 0.05), which suggests that the top fraction is cholesterol-enriched and contains the largest proportion of lipid rafts (Figure 18B). The non-raft fraction had decreased cholesterol per protein (not significant) compared with the PM fraction, which might indicate that separation of raft and non-raft membranes from the PM

fraction was successful. We also measured the opioid receptor localization in raft and non-raft fractions: the raft fraction had the highest proportion of mu-opioid receptors (11.02 ± 1.96 pmol/mg) compared with the PM (6.18 ± 0.86 pmol/mg) and non-raft (3.69 ± 0.51 pmol/mg) fractions (Figure 18C). Although this did not reach statistical significance by one-way ANOVA with Bonferroni's post-hoc test ($p = 0.0860$), this enrichment of mu receptors proposed in lipid rafts is consistent with the findings by Zheng et al. and currently-unpublished results from our lab (9). However, when receptor is analyzed per μg cholesterol, all fractions are approximately the same, indicating that mu receptors might associate with cholesterol, regardless of location in the cell membrane (Figure 18D).

Finally, we tested the function of adenylyl cyclase in each membrane fraction. In all fractions, forskolin was able to stimulate the production of cAMP indicating the presence of functional AC in all fractions (Figure 19).

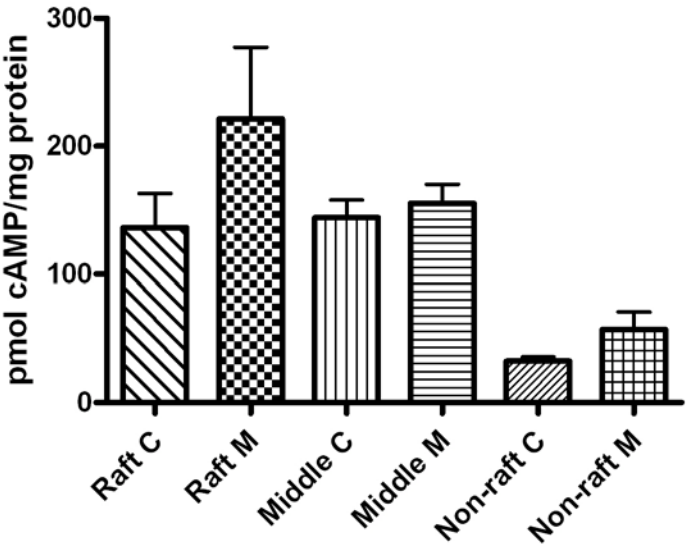

Figure 19. Raft fractions exhibit higher cAMP accumulation after precipitation of overshoot when compared with non-raft fractions. C6μ cells were incubated with or without 1 μM morphine in DMEM + FBS overnight (24 h) before starting the raft preparation protocol. Fractions isolated from cells incubated without morphine have the suffix "C" while fractions isolated from morphine-treated cells have the suffix "M." Overshoot was precipitated using naloxone in the presence of 5 μM forskolin. Data is presented as the mean pmol cAMP accumulation per mg protein ± S.E.M. (n = 4, in duplicate).

To measure expression of overshoot in all fractions, cells were pre-treated with 1 μM morphine overnight (24 h) before performing the raft preparation protocol the following day. Sensitization was induced by morphine instead of DAMGO to reduce internalization of receptors (35,36). Raft fractions had greater cAMP accumulation per protein after precipitation of overshoot with forskolin the presence of naloxone when compared with non-raft fractions. However, the % overshoot was approximately equal in all fractions (data not shown), indicating that the decrease in cAMP accumulation is the result of decreased AC levels in non-raft fractions rather than the absence of lipid rafts.

Discussion

The purpose of these studies was to understand the role of cholesterol and lipid rafts in adenylyl cyclase sensitization using both whole C6 cells expressing the mu-opioid receptor (C6μ) and membrane fractions isolated from C6μ cells. In the first set of experiments utilizing whole cells only, we found that cholesterol depletion affect the development phase of overshoot more than the expression phase. This conclusion was reached by showing that cAMP overshoot significantly decreased if cholesterol was depleted prior to development of sensitization of AC with chronic DAMGO treatment. However, because cholesterol levels remained low after chronic DAMGO treatment, we could also be affecting the expression phase of overshoot. Therefore, in the second set of experiments, we depleted cholesterol after chronic (overnight) DAMGO treatment so that we would only be affecting the expression phase. There was no change in cAMP production when overshoot from overnight DAMGO treatment was precipitated after cholesterol depletion compared to serum-free controls

We did notice, however, that overshoot decreased when cholesterol was depleted after 1 h chronic DAMGO treatment, though this might be due to differences in short- and long-term AC sensitization. There is evidence of protein expression changes that occur after long-term agonist treatment (37,38), which could make long-term sensitization more permanent and less sensitive to cholesterol effects. Ammer and Schulz found that chronic administration of morphine increased $G\alpha_s$ levels in SH-SY5Y cells which was required for expression of overshoot and was mediated by the mu-receptor (37,38). In HEK cells expressing D_4 dopamine receptors, $G\alpha_i$, has also been shown to be down-regulated following long-term (18 h) but not short-term (2 h) quinpirole treatment (39).

We optimized the protocol by Smart et al. (15) because previously published methods were not ideal for separating rafts for functional studies (12,40). Membranes isolated using the

optimized raft separation protocol also supported our findings that cholesterol is important in AC sensitization. We were able to achieve some separation of cholesterol-enriched membranes and showed that these fractions contained higher levels of mu-opioid receptor per mg protein, which agrees with previously published results (9). In addition, we were also able to show that cholesterol-enriched fractions were enriched in AC and that AC could be sensitized in fractions isolated from cells treated overnight with morphine. However, the finding that overshoot was similar in all fractions also supported our hypothesis that expression of overshoot is not dependent on lipid rafts because AC was sensitized in whole cells prior to the raft separation protocol and expression of overshoot was similar in raft and non-raft fractions. We were unable, however, to obtain relatively pure raft and non-raft fractions as indicated by western blotting of raft and non-raft markers. Nevertheless, the optimized detergent-free protocol yielded functional membranes and preserved cholesterol and receptor enrichment in raft fractions. Compared with traditionally used methods to isolate rafts, this method is milder and has been shown to preserve enzyme activity and raft purity (15,41,42). The reduction of sucrose in comparison to traditional raft separation methods is also important, as previous studies have shown that sucrose can increase the number of surface receptors, as well as the amount of agonist needed to sensitize adenylyl cyclase by inhibition of receptor endocytosis (43,44). The raft preparation AC overshoot results, along with the whole-cell cholesterol depletion results, suggest that the integrity of cholesterol-enriched membrane domains is important in mu-opioid receptor signaling to AC.

Macdonald and Pike (42) have recently reported another detergent-free raft separation method based on the protocol by Smart et al. as well (42). The method by Macdonald and Pike also eliminated the second 90 min spin, and further reduced the overall protocol time by

eliminating the plasma membrane separation step. However, the membrane fractions isolated by Macdonald and Pike were not tested for functionality and signal ratios of caveolin to transferrin varied depending on the cell type used (42). Morris et al. used the raft separation protocol of Macdonald and Pike (42) to show that α-adrenergic receptors in rat fibroblasts are localized in rafts and exit these rafts following agonist stimulation (45).

One of the major difficulties that we encountered throughout the optimization of the protocol by Smart et al. was the high variability between replicate experiments. Even membranes isolated using well-established protocols, such as those utilizing Triton X-100 can have inconsistencies. For instance, Wang et al. showed that COS-1 cells expressing Lck-derived N-terminal acylated green fluorescent protein (GFP) had a 61% association in lipid rafts isolated using Triton X-100 (46). However, McCabe and Berthiaume also utilized Triton X-100 to but showed that the same acylated GFP construct did not associate with rafts (47). These discrepancies may be the result of variable lipid ratios in different cells that are unaccounted for when using a static raft preparation protocol (48). Also, because all current raft separation methods require agitation of plasma membranes to fragment raft and non-raft domains, the integrity of isolated fractions is a possible concern. An alternative to physical separation of rafts in density gradients is the use of biophysical methods that utilize whole cells. FRET (fluorescence resonance energy transfer) has been used to visualize co-localization of raft markers such as ganglioside GM1 with membrane proteins (49). Immunostaining with cholera toxin B, which binds selectively to GM1, and confocal microscopy can be used to observe co-localization (50). Newer single-molecule fluorescence techniques such as STORM (stochastic optical reconstruction microscopy) can distinguish real-time localization of signals to within 1 nm, well within the hypothesized caveolae dimensions (~25-100 nm), and can allow for the

construction of three-dimensional images (51,52). Other techniques that do not require the use of fluorescent dyes, such as atomic force microscopy, are able to measure the formation and dynamics of membrane microdomains under physiological conditions, though identification of membrane-bound proteins may be difficult (53).

Previous studies have investigated the role of cholesterol and lipid rafts in mu-opioid signaling and sensitization. Zhao et al. have demonstrated that in HEK293 cells, mu opioid receptors are localized in cholesterol-rich domains and that cholesterol is needed for mu-opioid receptor-mediated overshoot (6). Mu-opioid receptor localization in lipid rafts might result from direct receptor interactions with caveolin via several proposed caveolin binding motifs (54). Alternatively, mu-opioid receptor localization in cholesterol-enriched domains may be due to the association of receptor with G proteins. Following morphine treatment, movement of $G\alpha_{i2}$ out of rafts occurred along with translocation of mu-opioid receptors out of rafts, suggesting that interactions between mu receptors and G proteins might mediate localization in rafts (9). Furthermore, mu-opioid receptors have been found to depend on cholesterol for coupling to G proteins (55). In addition, data from our lab has shown that cholesterol depletion of HEK FLAG-mu cells using MβCD reduced the potency of selective mu agonist DAMGO to activate G proteins, and produced a low-affinity agonist binding site similar to the site induced by decoupling of the Gα subunit from mu-opioid receptors using NaCl and GTPγS (unpublished results). In contrast, a study by Emmerson et al. demonstrated that increasing membrane rigidity by addition of cholesterol hemisuccinate increased DAMGO and sufentanil (mu-opioid agonist) binding affinity and that the effect is not dependent on a direct cholesterol-receptor interactions (56). These previous findings support the results presented here that mu-opioid receptor number

per μg cholesterol was equivalent across all fractions likely because mu-opioid receptors require cholesterol for functionality.

Lipid rafts and cholesterol have also been implicated in the function of other G protein-coupled receptors (GPCRs) and components of GPCR signaling cascades. Modulation of receptor function by changes in membrane fluidity have also been confirmed with β-adrenergic (57) and muscarinic acetylcholine (58) receptors. In addition to mu-opioid receptors, kappa-opioid (59), β-adrenergic (β-AR) (45), P2Y purinergic (60) and muscarinic acetylcholine receptors (60,61) have also been shown to associate with rafts. Moffet et al. showed that palmitoylation and myristoylation were necessary for the translocation of $G\alpha_i$ into rafts, suggesting that targeting of G proteins to raft domains might be dependent on fatty acylation (62). Caveolin also contains binding domains that interact with $G\alpha_s$, $G\alpha_i$ and $G\alpha_o$ and might regulate G protein activity (63). As mentioned earlier, AC5 and AC6 (1,6) are localized in rafts, while $G\alpha_{i/o}$, $G\beta\gamma$ (7) and Raf-1, move to rafts following activation (8). In addition, protein kinase C (PKC) was also shown to be localized in rafts along with other components of the extracellular signal-regulated protein kinase (ERK) cascade (3). PKC is also recruited to rafts following purinergic stimulation in glial cells (60) and is inhibited by caveolin-1 (64). Activation of PKC has been shown to enhance the activity of multiple isoforms of AC (1). Protein kinase A (PKA), which can be localized with caveolin (65) and whose activation leads to inhibition of AC 5 and AC6 activity (2), is also inhibited by caveolin-1 (66). In CAD cells expressing D_2 receptors, chronic treatment with PKA inhibitors sensitized AC6, while chronic treatment with PKA activators reduced agonist-induced sensitization (67). While G proteins and other signaling molecules have been shown to associate with rafts, the mechanisms of interaction are still unclear. For instance, Ostrom et al. demonstrated that overexpression of AC6 in cardiac myocytes, which was localized

with caveolin, did not increase cAMP production, suggesting that observing protein levels in rafts may not be enough to explain cellular responses to stimuli (68).

In conclusion, these studies highlight the importance of cholesterol in understanding mechanisms of mu-opioid receptor-mediated adenylyl cyclase sensitization. Our initial experiments with whole cells demonstrated that the role of cholesterol in the development and expression phases of overshoot is complex and prompted further investigation into the composition and function of lipid rafts. Analysis of isolated raft membranes, using a detergent-free protocol to preserve integrity of membrane proteins, confirmed previous findings that mu-opioid receptors are localized in rafts and provided evidence supporting the hypothesis that cholesterol is required for mu-opioid receptor function. While the clinical significance of chronic opioid-induced sensitization has been established (69-71), the effects of cholesterol on physiological responses to opioid use have not been investigated. This is especially important because of continuously lowering clinical cholesterol goals (72).

Terms and Abbreviations

GPCR – G protein-coupled receptor

AC – adenylyl cyclase

DMEM – Dulbecco's Modified Eagle Medium

C6μ – C6 rat glioma cells stably expressing the mu-opioid receptor (rat)

[^{35}S]GTPγS - guanosine 5'-O-[gamma-thio]triphosphate (nonhydrolyzable GTP analog)

MβCD – methyl-β-cyclodextrin

MβCD/chol – 4 mM MβCD with cholesterol included as suspension

MβCD-CH – 4 mM MβCD:cholesterol complex (8:1)

DAMGO – [D-Ala^2, N-MePhe^4, Gly-ol]-enkephalin

MAPK – mitogen-activated protein kinase

ERK – extracellular signal-regulated kinase

EEA1 – Early Endosome Antigen 1

PM – plasma membrane

PNS – postnuclear supernatant

Acknowledgments

Thank you to Dr. John Traynor for
giving me the opportunity to work in his lab
and for challenging me these past 2 years

Special thank you to Erica Levitt for
her continual support, her expertise on the
effects of cholesterol depletion and for her
invaluable suggestions about my thesis drafts

Special thank you to Mary Clark (Satin Lab)
for introducing me to the field of opioid receptor
signaling and providing me much-needed guidance
and encouragement towards my project
throughout the entire process

References

1. Watts, V. J., and Neve, K. A. (2005) *Pharmacol. Ther.* **106**, 405-421
2. Chen, Y., Harry, A., Li, J., Smit, M. J., Bai, X., Magnusson, R., Pieroni, J. P., Weng, G., and Iyengar, R. (1997) *Proc. Natl. Acad. Sci. U. S. A.* **94**, 14100-14104
3. Rybin, V. O., Xu, X., and Steinberg, S. F. (1999) *Circul. Res.* **84**, 980-988
4. Ostrom, R. S., and Insel, P. A. (2004) *Br. J. Pharmacol.* **143**, 235-245
5. Allen, J. A., Halverson-Tamboli, R. A., and Rasenick, M. M. (2007) *Nat Rev Neurosci* **8**, 128-140
6. Zhao, H., Loh, H. H., and Law, P. Y. (2006) *Mol. Pharmacol.* **69**, 1421-1432
7. Bayewitch, M. L., Nevo, I., Avidor-Reiss, T., Levy, R., Simonds, W. F., and Vogel, Z. (2000) *Mol. Pharmacol.* **57**, 820-825
8. Mineo, C., James, G. L., Smart, E. J., and Anderson, R. G. (1996) *J. Biol. Chem.* **271**, 11930-11935
9. Zheng, H., Chu, J., Qiu, Y., Loh, H. H., and Law, P. Y. (2008) *Proc. Natl. Acad. Sci. U. S. A.* **105**, 9421-9426
10. Chang, W. J., Ying, Y. S., Rothberg, K. G., Hooper, N. M., Turner, A. J., Gambliel, H. A., De Gunzburg, J., Mumby, S. M., Gilman, A. G., and Anderson, R. G. (1994) *J. Cell Biol.* **126**, 127-138
11. Sargiacomo, M., Sudol, M., Tang, Z., and Lisanti, M. P. (1993) *The Journal of cell biology* **122**, 789-807
12. Brown, D. A., and Rose, J. K. (1992) *Cell* **68**, 533-544
13. Lichtenberg, D., Goni, F. M., and Heerklotz, H. (2005) *Trends Biochem. Sci.* **30**, 430-436
14. Chamberlain, L. H. (2004) *FEBS Lett.* **559**, 1-5
15. Smart, E. J., Ying, Y. S., Mineo, C., and Anderson, R. G. (1995) *Proc. Natl. Acad. Sci. U. S. A.* **92**, 10104-10108
16. Clark, M. J., Harrison, C., Zhong, H., Neubig, R. R., and Traynor, J. R. (2003) *J. Biol. Chem.* **278**, 9418-9425
17. Christian, A., Haynes, M., Phillips, M., and Rothblat, G. (1997) *J. Lipid Res.* **38**, 2264-2272
18. Laemmli, U. K. (1970) *Nature* **227**, 680-685
19. Ostermeyer, A. G., Beckrich, B. T., Ivarson, K. A., Grove, K. E., and Brown, D. A. (1999) *J. Biol. Chem.* **274**, 34459-34466
20. Ilangumaran, S., and Hoessli, D. C. (1998) *Biochem. J.* **335**, 433-440
21. Clark, M. J., and Traynor, J. R. (2006) *J. Neurochem.* **99**, 1494-1504
22. Bradford, M. M. (1976) *Anal. Biochem.* **72**, 248-254
23. Harder, T., Scheiffele, P., Verkade, P., and Simons, K. (1998) *J. Cell Biol.* **141**, 929-942
24. Rego, A. C., Vesce, S., and Nicholls, D. G. (2001) *Cell Death Differ.* **8**, 995-1003
25. Prpic, V., Green, K., Blackmore, P., and Exton, J. (1984) *J. Biol. Chem.* **259**, 1382-1385
26. Song, C. S., Rubin, W., Rifkind, A. B., and Kappas, A. (1969) *J. Cell Biol.* **41**, 124-132
27. Head, B. P., Patel, H. H., Roth, D. M., Murray, F., Swaney, J. S., Niesman, I. R., Farquhar, M. G., and Insel, P. A. (2006) *J. Biol. Chem.* **281**, 26391-26399
28. Plowman, S. J., Muncke, C., Parton, R. G., and Hancock, J. F. (2005) *Proc. Natl. Acad. Sci. U. S. A.* **102**, 15500-15505
29. Balbis, A., Parmar, A., Wang, Y., Baquiran, G., and Posner, B. I. (2007) *Endocrinology* **148**, 2944-2954

30. Sharma, D. K., Choudhury, A., Singh, R. D., Wheatley, C. L., Marks, D. L., and Pagano, R. E. (2003) *J. Biol. Chem.* **278**, 7564-7572
31. Allen, J. A., Yu, J. Z., Donati, R. J., and Rasenick, M. M. (2005) *Mol. Pharmacol.* **67**, 1493-1504
32. Furuchi, T., and Anderson, R. G. W. (1998) *J. Biol. Chem.* **273**, 21099-21104
33. Liu, P., Ying, Y.-s., and Anderson, R. G. W. (1997) *Proc. Natl. Acad. Sci. U. S. A.* **94**, 13666-13670
34. Di Guglielmo, G. M., Le Roy, C., Goodfellow, A. F., and Wrana, J. L. (2003) *Nat Cell Biol* **5**, 410-421
35. Yabaluri, N., and Medzihradsky, F. (1997) *Mol. Pharmacol.* **52**, 896-902
36. Wang, Y., Van Bockstaele, E. J., and Liu-Chen, L.-Y. (2008) *Life Sci.* **83**, 693-699
37. Ammer, H., and Schulz, R. (1996) *Brain Res.* **707**, 235-244
38. Ammer, H., and Schulz, R. (1993) *Biochem. J.* **295**, 263-260
39. Watts, V. J., Vu, M. N., Wiens, B. L., Jovanovic, V., Van Tol, H. H. M., and Neve, K. A. (1999) *Psychopharmacology (Berl).* **141**, 83-92
40. Song, K. S., Li, S., Okamoto, T., Quilliam, L. A., Sargiacomo, M., and Lisanti, M. P. (1996) *J. Biol. Chem.* **271**, 9690-9697
41. Shogomori, H., and Brown, D. A. (2003) *Biol. Chem.* **384**, 1259-1263
42. Macdonald, J. L., and Pike, L. J. (2005) *J. Lipid Res.* **46**, 1061-1067
43. Heuser, J., and Anderson, R. (1989) *J. Cell Biol.* **108**, 389-400
44. Corbani, M., Gonindard, C., and Meunier, J.-C. (2004) *Endocrinology* **145**, 2876-2885
45. Morris, D. P., Lei, B., Wu, Y.-X., Michelotti, G. A., and Schwinn, D. A. (2008) *J. Biol. Chem.* **283**, 2973-2985
46. Wang, T.-Y., Leventis, R., and Silvius, J. R. (2001) *Biochemistry (Mosc).* **40**, 13031-13040
47. McCabe, J. B., and Berthiaume, L. G. (2001) *Mol. Biol. Cell* **12**, 3601-3617
48. Edidin, M. (2003) *Annu. Rev. Biophys. Biomol. Struct.* **32**, 257-283
49. Kenworthy, A. K., Petranova, N., and Edidin, M. (2000) *Mol. Biol. Cell* **11**, 1645-1655
50. Fra, A., Williamson, E., Simons, K., and Parton, R. (1994) *J. Biol. Chem.* **269**, 30745-30748
51. Huang, B., Wang, W., Bates, M., and Zhuang, X. (2008) *Science* **319**, 810-813
52. Duggan, J., Jamal, G., Tilley, M., Davis, B., McKenzie, G., Vere, K., Somekh, M., O'Shea, P., and Harris, H. (2008) *Eur. Biophys. J.* **37**, 1279-1289
53. Connell, S. D., and Smith, D. A. (2006) *Mol. Membr. Biol.* **23**, 17 - 28
54. Couet, J., Li, S., Okamoto, T., Ikezu, T., and Lisanti, M. P. (1997) *J. Biol. Chem.* **272**, 6525-6533
55. Gaibelet, G., Millot, C., Lebrun, C., Ravault, S., SauliÃ¨re, A., AndrÃ©, A., Lagane, B., and Lopez, A. (2008) *Mol. Membr. Biol.* **25**, 423 - 435
56. Emmerson, P. J., Clark, M. J., Medzihradsky, F., and Remmers, A. E. (1999) *J. Neurochem.* **73**, 289-300
57. Ben-Arie, N., Gileadi, C., and Schramm, M. (1988) *Eur. J. Biochem.* **176**, 649-654
58. Berstein, G., Haga, T., and Ichiyama, A. (1989) *Mol. Pharmacol.* **36**, 601-607
59. Xu, W., Yoon, S.-I., Huang, P., Wang, Y., Chen, C., Chong, P. L.-G., and Liu-Chen, L.-Y. (2006) *J. Pharmacol. Exp. Ther.* **317**, 1295-1306
60. Weerth, S. H., Holtzclaw, L. A., and Russell, J. T. (2007) *Cell Calcium* **41**, 155-167
61. Dessy, C., Kelly, R. A., Balligand, J. L., and Feron, O. (2000) *EMBO J.* **19**, 4272-4280

62. Moffett, S., Brown, D. A., and Linder, M. E. (2000) *J. Biol. Chem.* **275**, 2191-2198
63. Li, S., Okamoto, T., Chun, M., Sargiacomo, M., Casanova, J. E., Hansen, S. H., Nishimoto, I., and Lisanti, M. P. (1995) *J. Biol. Chem.* **270**, 15693-15701
64. Shakirova, Y., Bonnevier, J., Albinsson, S., Adner, M., Rippe, B., Broman, J., Arner, A., and Sward, K. (2006) *Am J Physiol Cell Physiol* **291**, C1326-1335
65. Sampson, L. J., Hayabuchi, Y., Standen, N. B., and Dart, C. (2004) *Circul. Res.* **95**, 1012-1018
66. Engelman, J. A., Chu, C., Lin, A., Jo, H., Ikezu, T., Okamoto, T., Kohtz, D. S., and Lisanti, M. P. (1998) *FEBS Lett.* **428**, 205-211
67. Johnston, C. A., Beazely, M. A., Vancura, A. F., Wang, J. K. T., and Val J. Watts. (2002) *J. Neurochem.* **82**, 1087-1096
68. Ostrom, R. S., Violin, J. D., Coleman, S., and Insel, P. A. (2000) *Mol. Pharmacol.* **57**, 1075-1079
69. Bie, B., Peng, Y., Zhang, Y., and Pan, Z. Z. (2005) *J. Neurosci.* **25**, 3824-3832
70. Chu, L. F., Angst, M. S., and Clark, D. (2008) *The Clinical Journal of Pain* **24**, 479-496
71. Nestler, E. J., and Aghajanian, G. K. (1997) *Science (New York, N.Y.)* **278**, 58-63
72. Smith, S. C., Jr, Allen, J., Blair, S. N., Bonow, R. O., Brass, L. M., Fonarow, G. C., Grundy, S. M., Hiratzka, L., Jones, D., Krumholz, H. M., Mosca, L., Pasternak, R. C., Pearson, T., Pfeffer, M. A., and Taubert, K. A. (2006) *J. Am. Coll. Cardiol.* **47**, 2130-2139